

A Tutorial on Selectivity Determination in C(sp²)-H Oxidative Addition of Arenes by Transition Metal Complexes

Tyler P. Pabst and Paul J. Chirik*



Cite This: *Organometallics* 2021, 40, 813–831



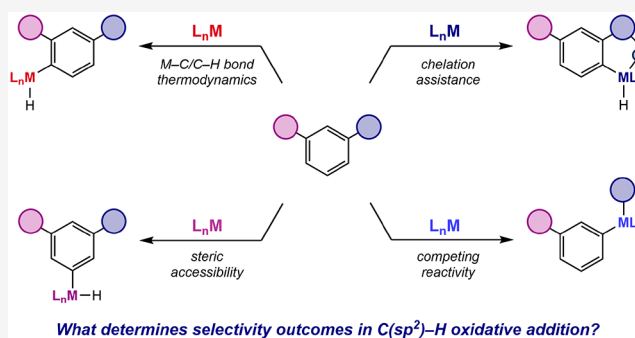
Read Online

ACCESS |

Metrics & More

Article Recommendations

ABSTRACT: A Tutorial on factors that determine the selectivity in C(sp²)-H activation and functionalization reactions involving two-electron oxidative addition processes with transition metals is presented. The interplay of the thermodynamics of C(sp²)-H oxidative addition and kinetic influences upon regioselectivity are presented alongside pedagogically valuable experimental and computational results from the literature. Mechanisms and energetics of chelate-assisted C(sp²)-H oxidative addition are examined, as are concepts related to chemoselectivity in the oxidative addition of C(sp²)-H or C(sp²)-X (X = F, Cl, Br, I) bonds with aryl halide substrates.



INTRODUCTION

The selective functionalization of unactivated carbon-hydrogen bonds has long been recognized for its potential to transform synthetic chemistry and has emerged as a frontier research area in organometallic chemistry.¹ C-H functionalization earns this distinction because of the ubiquity of these bonds in organic molecules and their typical recalcitrance to reactivity. If selective reactions are realized, there is tremendous potential as a retrosynthetic tool as well as in the transformation of commodity feedstocks. Historically, organometallic chemists have embraced the challenge associated with breaking strong bonds; accordingly, the systematic study of intermolecular C-H activation began primarily with efforts toward transition-metal-mediated activation of pure hydrocarbons, with a specific emphasis on methane.² Over time, lessons from these fundamental studies evolved into a broader synthetic strategy for the selective elaboration of C-H bonds in complex organic molecules and has since been applied as a transformative tool in late-stage functionalization. Many reviews on these topics have been published, including a special issue of *Chemical Reviews*.³

Given that C-H bonds are ubiquitous in organic compounds and often have similar properties (e.g. bond strength, polarity, acidity), both chemo- and regioselectivity are paramount in C-H bond functionalization reactions. The utility of any C-H activation and functionalization method is reliant on the ability to select for a desired C-H bond in the presence of others. This is especially important for applications in late-stage functionalization, where the number of chemically similar C-H bonds is typically large even for relatively small molecules.⁴ All forms of selectivity—chemoselectivity, regio-

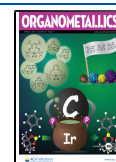
selectivity, and stereoselectivity—are the result of the relative energetics of a given pathway in comparison to the others that are possible in the system of interest. For this reason, the factors that determine the selectivity in a chemical reaction are best addressed through an analysis of the accepted mechanism and consideration of the thermodynamic and kinetic preferences of the given system.

In this Tutorial, these concepts are addressed in the specific context of C(sp²)-H functionalization, a subfield with widespread application in pharmaceutical, agrochemical, and materials chemistry. The scope of the Tutorial is confined to reactions whereby the C-H bond cleavage likely or is generally accepted to occur by two-electron oxidative addition.

What factors contribute to selectivity outcomes in C(sp²)-H oxidative addition of an aromatic compound? In the simplest case of a monosubstituted arene, three distinct C(sp²)-H bond environments exist at the positions *ortho*, *meta*, and *para* to the (non-hydrogen) substituent (Figure 1). Depending upon its identity, this substituent may perturb the electronic and steric environments at each site, potentially distinguishing C(sp²)-H bonds by their strengths or acidities. These perturbations give rise to intrinsic thermodynamic or kinetic preferences for oxidative addition at one site or another. Some substituents may impact regioselectivity for steric

Received: January 15, 2021

Published: March 16, 2021



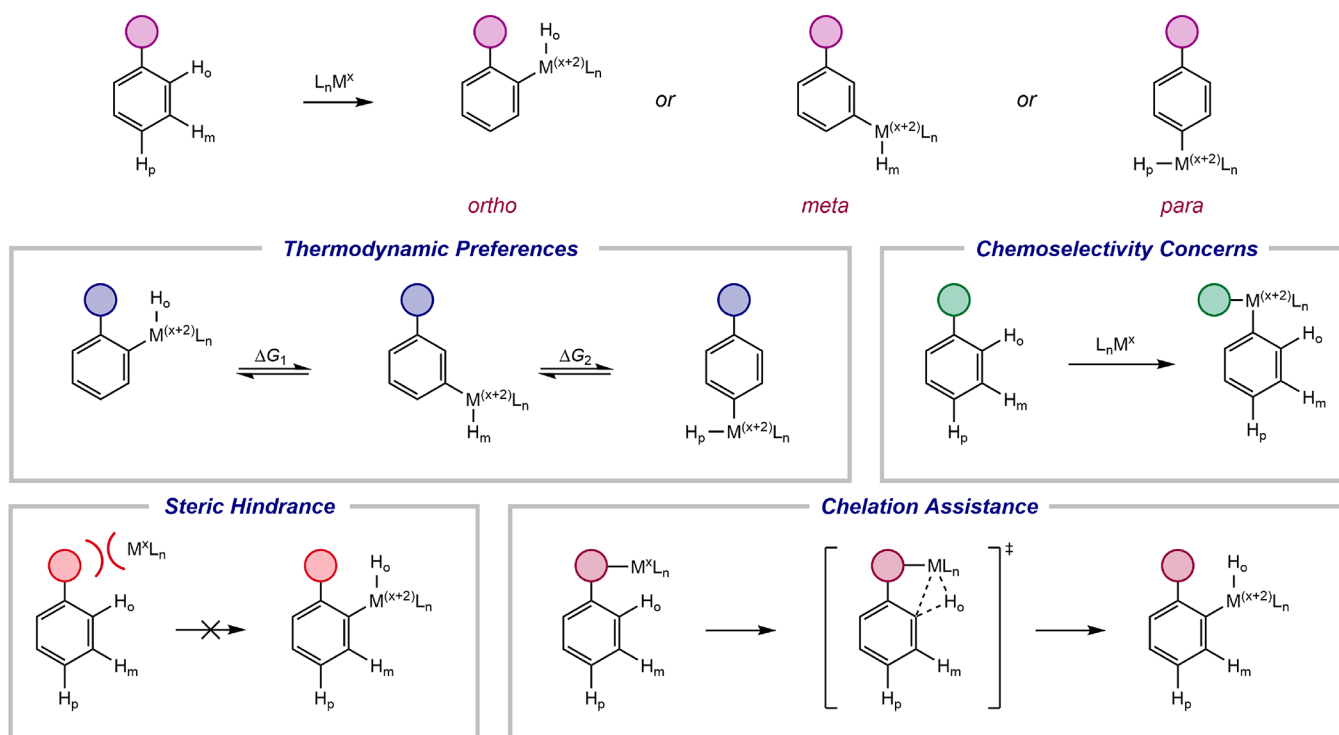


Figure 1. Selected factors influencing selectivity outcomes in $C(sp^2)$ -H oxidative addition.

reasons, either by blocking adjacent positions or by serving as a chelating directing group, the latter approach being a commonly employed strategy for regioselective C-H functionalization.⁵ The chemoselectivity of oxidative addition is also of interest, as chemical bonds other than C-H (particularly C-X; X = halogen) often are more reactive with reduced metal complexes.²

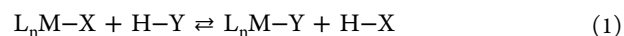
In this Tutorial, the concepts that determine regio- and chemoselectivity in $C(sp^2)$ -H oxidative addition reactions are explored in the context of subsequent catalytic functionalization. Because Tutorials are focused on pedagogy and are not intended to be comprehensive reviews,⁶ selected representative literature examples are presented to illustrate the various concepts. By emphasizing the underlying mechanistic and energetic concepts, we hope to provide important guiding principles for understanding the selectivity of various metal-catalyzed arene functionalization reactions.

■ THERMODYNAMICS OF C-H OXIDATIVE ADDITION

The Bryndza-Bercaw Relation: Correlation of M-X and H-X Bond Strengths. At first glance, it may seem intuitive for weaker C-H bonds to be preferentially activated over stronger ones. However, this is often not the case, as the thermodynamics of C-H activation often favor cleavage of the stronger C-H bond,⁷ one of the distinguishing features of the field since its inception. To rationalize these observations, bond dissociation (free) energy correlations and their visual representations are instructive, and several notable examples from the literature will be presented. While bond dissociation enthalpy (BDE) has historically been employed as a measure of bond strength, bond dissociation free energy (BDFE) has become increasingly more common and is preferred in transition-metal chemistry when the entropic data are available;⁸ in discussions of previously published studies, the

thermodynamic metric employed will be explicitly noted. For each analysis, the values and trends reported by the original authors of each cited work will be used, even though the accepted value for a given BD(F)E can change as new methods for their determination or calculation are introduced.⁹

In an early systematic study of BDE correlations, Bryndza, Bercaw, and co-workers experimentally determined the value of the equilibrium constant for the reaction presented in eq 1 and applied this information to establish a relationship between the relative BDEs of M-X and H-X bonds.¹⁰ While there have been notable deviations from and revisions to this model, we maintain the use of the “Bryndza-Bercaw relation” for conceptual and historical reasons. In these investigations, two families of complexes, $(dpppe)Pt(Me)X$ and $(\eta^5-C_5Me_5)Ru(PMe_3)_2X$, were used to systematically evaluate the thermochemistry of this reaction for a series of X and Y ligands including hydride, alkyl, alkoxy, amide, and others. A plot of the relative H-X BDEs versus the corresponding M-X BDEs established a linear correlation with a slope near unity (Figure 2). This is to say that, for the complexes examined, the relative H-X BDEs and the relative M-X BDEs correlate sufficiently to enable prediction of a particular BDE, given knowledge of the correlated value. Simply stated, these late-transition-metal complexes “behave like large hydrogen atoms in terms of binding organic radical fragments”.¹¹ This 1:1 correlation is a powerful concept when it is applied to the prediction of transition M-X BDEs, which are often more challenging to obtain experimentally in comparison to those for the corresponding H-X bonds.³⁸



Deviations from the 1:1 relationship have been observed, and their significance is noteworthy. A standard convention adopted after the work of Bryndza and Bercaw places the relative values for H-X bond energies on the x axis and those

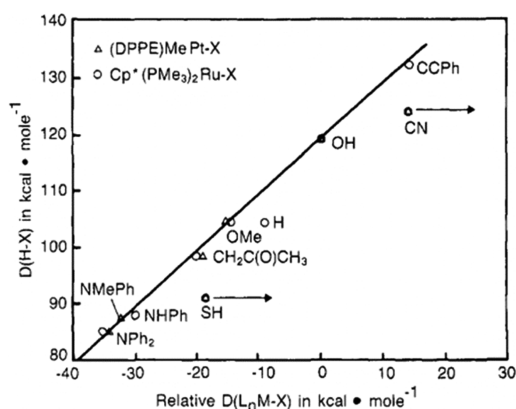


Figure 2. Relative bond dissociation enthalpies (BDEs) of H–X vs L_n M–X bonds with all values given in kcal/mol. The M–O BDE of L_n M–OH was arbitrarily assigned a relative value of 0.0 kcal/mol, and a line with an arbitrary slope of 1.0 was drawn through the data point for which X = OH. Arrows for X = SH, CN indicate an experimentally established lower bound for these values. Reproduced with permission from ref 10. Copyright 1987 American Chemical Society.

of the M–X bonds on the y axis, and this convention will be used going forward. A slope greater than unity implies that M–X bonding is more sensitive than H–X bonding for a given series of X ligands, whereas a slope less than unity would indicate more favorable H–X bonding in comparison to M–X bonding (Figure 3).

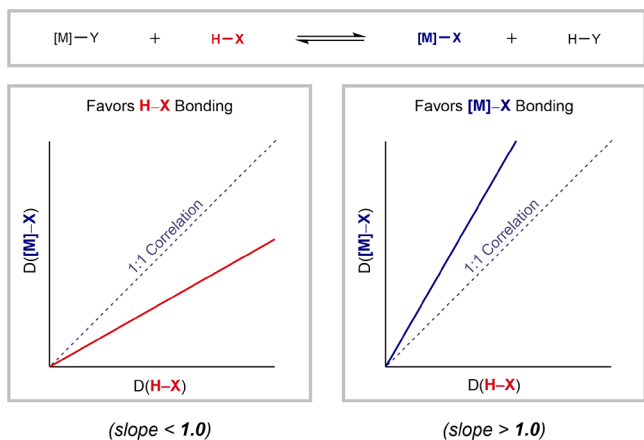


Figure 3. Hypothetical BDE (or BDFE) correlation diagrams displaying deviations from the 1:1 correlation first established by Bryndza and Bercau (see refs 10 and 11).

Metal hydrides exhibit notable deviations from the 1:1 correlation,^{9,11,12} such as in the case where X = H.¹³ Plots of M–X vs H–X BDEs reveal that the point for X = H “consistently falls off the line in the direction of stronger L_n M–H” (Figure 2).¹³ Labinger and Bercau discussed the origins of this exception, beginning with a fundamental question: does the correlation “fail” at X = H because M–H is anomalously strong or because H–H is anomalously weak? The latter case is true; on the basis of fundamental electronegativity arguments, the M–H bond is polarized to a greater extent in comparison to the covalent bond of H_2 .¹⁴ The H–H bond exhibits the minimal amount of ionic character among the series of “H–X” bonds, rendering it weaker than anticipated from the BDE of M–H. For polyatomic fragments including

transition-metal complexes, this explanation uses the *elemental* electronegativity of the atom involving in bonding rather than the *group* electronegativity of the fragment; Wolczanski and co-workers have articulated the caveats of this simplification.¹⁵

Other deviations from a 1:1 correlation have been identified and are dependent upon the specific metal complex examined. Anderson, Bergman, and co-workers investigated the series of nickel amide complexes $(\eta^5-C_5Me_5)Ni(PET_3)NHAr$, where the aryl amide was varied by the identity of the substituent at the 4-position of the ring.¹⁶ The correlation between Ni–N and H–N BDEs is strong, and a slope of approximately 1.9 was reported (Figure 4). Introduction of electron-withdrawing

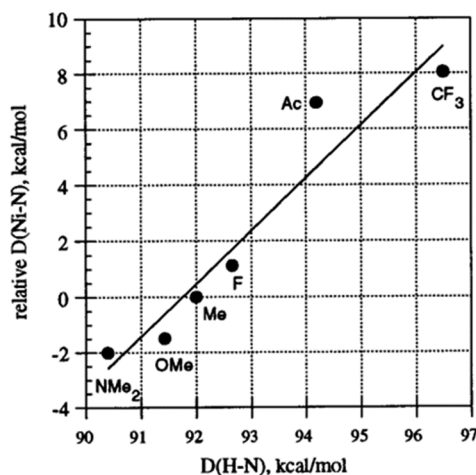


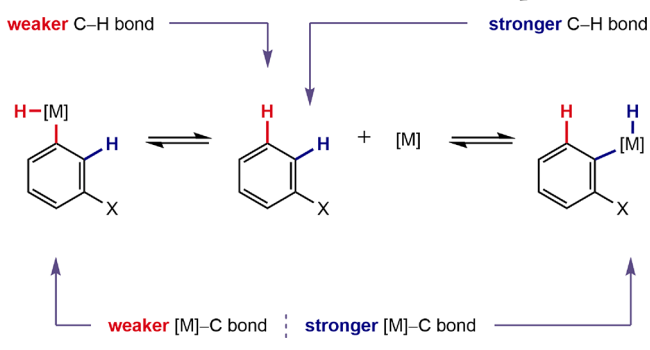
Figure 4. Plot of relative Ni–N BDEs in $(\eta^5-C_5Me_5)Ni(PET_3)NH(4-C_4H_4X)$ versus H–N BDEs in the corresponding anilines with a best-fit line of slope 1.9. The data points are labeled with the identity of the “X” substituent of the aniline. Reproduced with permission from ref 16. Copyright 1997 American Chemical Society.

substituents on the amide aryl ring favored M–X bonding, while electron-donating groups favored H–X bonding. These trends were rationalized on the basis of the ionicity or covalency of the interactions; additionally, the introduction of electron-withdrawing groups lowers the energy of the nitrogen lone pair of the amide ligand, diminishing unfavorable interactions between these electrons and those of the filled Ni d orbitals.

M–C/C–H Bond Energy Correlations: Application to C–H Activation Selectivities. For an analysis of the energetics of C–H activation reactions and translation onto observed regioselectivities, “X” and “Y” fragments in eq 1 are replaced with aryl fragments arising from oxidative addition of a generic monosubstituted arene (Scheme 1). The specific identity of the aryl substituent is unimportant; what is important is the presence of two electronically distinct C–H bonds that can undergo activation by the metal. The C–H bond strengths are not identical, although they are likely similar. What determines the position of this equilibrium?

First, it should be noted that the bond dissociation free energy of the metal–hydride interaction likely varies little with the connectivity of an alkyl or aryl ligand.¹⁷ Accordingly, the major contributors to the value of ΔG (and therefore the thermodynamic preference of the oxidative addition) are the metal–carbon and carbon–hydrogen bond strengths. In general, a stronger C–H bond translates to a stronger M–C bond following oxidative addition; thus, the formation of the

Scheme 1. Equilibrium for the Oxidative Addition of Two Different C–H Bonds to a Generic Metal Complex [M]



stronger M–C bond (compared to the M–C bond drawn on the opposite side of the equilibrium) necessarily arises from the cleavage of the stronger C–H bond in the substrate. To determine the position of the equilibrium depicted in Scheme 1, the sensitivity of the M–C or C–H BDEs (or BDFEs) to the identity of the organic fragment are important. This is precisely the question that can be addressed by bond energy correlation studies; that is, is the slope of $\Delta\text{BDE}(\text{M}-\text{C})$ vs $\Delta\text{BDE}(\text{C}-\text{H})$ greater than or less than 1.0?

Two independent and seminal studies by Jones and Wolczanski probed the direction and magnitude of M–C/C–H bond energy correlations.^{7,18,19} Because previous studies by Jones and Feher on C–H oxidative addition to $(\eta^5\text{-C}_5\text{Me}_5)\text{Rh}(\text{PMe}_3)$ demonstrated a thermodynamic preference for the activation of benzene over propane,²⁰ additional studies were undertaken to establish the kinetic and thermodynamic regioselectivity of C–H oxidative addition of various hydrocarbons. Photolysis of $\text{Tp}'\text{Rh}(\text{CNR})(\text{PhN}=\text{C}=\text{NR})$ (R = neopentyl) resulted in dissociation of the carbodiimide ligand and generated the rhodium complex active for C–H bond cleavage.^{8,18} Correlation of the M–C and H–C bond dissociation energies using exclusively experimentally determined values demonstrated a systematic deviation from the 1:1 relationship (Figure 5). The value of 1.22 obtained for the slope of the correlation indicates that the relative Rh–C bond

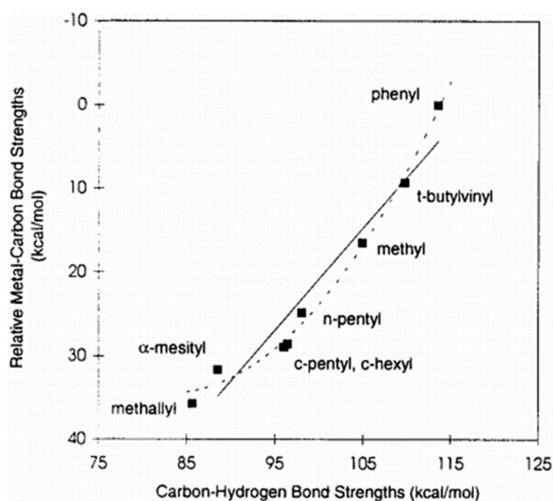


Figure 5. Plot of relative Rh–C bond strengths in $\text{Tp}'\text{Rh}(\text{CNNp})\text{-(H)(R)}$ versus C–H bond strengths in the corresponding hydrocarbons. Reproduced with permission from ref 7. Copyright 1999 American Chemical Society.

strengths are consistently more sensitive to the identity of the hydrocarbon ligand than those of the corresponding C–H bonds for the series of alkyl and aryl complexes evaluated.

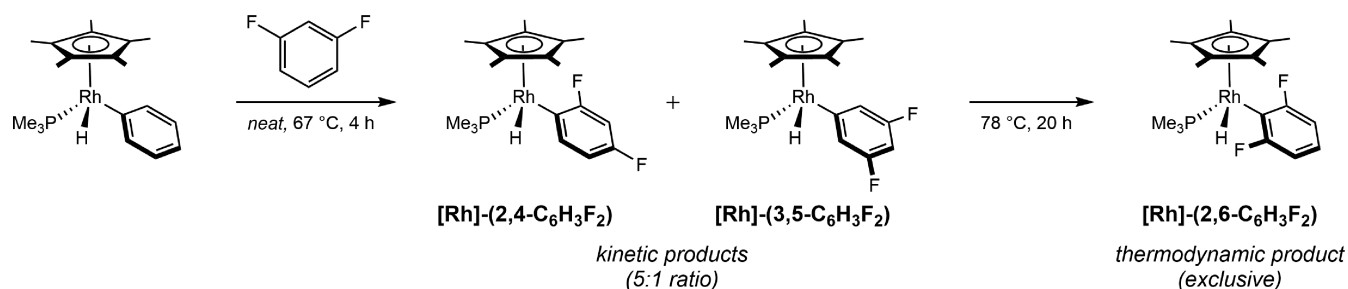
A similar result was obtained by Wolczanski and co-workers in the context of 1,2-addition and its microscopic reverse, 1,2-elimination of alkanes to early transition metals, chemistry detailed in a previous Tutorial.⁹ A comparison of the relative Ti–C bond strengths in $(\text{tBu}_3\text{SiO})_2(\text{tBu}_3\text{SiNH})\text{TiR}$ to those of the C–H bonds in the corresponding hydrocarbons produced a slope of 1.12 in the original publication, again favoring metal–carbon bonding.¹⁹ In the Wolczanski Tutorial, these correlations were regenerated using updated BDEs for the hydrocarbons, for which the accepted values had been revised since the initial report. The slope of the correlation obtained from new values was 0.97 and was further reduced to 0.77 upon removal of data points involving benzylic fragments.⁹ This significant change in the M–C/C–H relationship illustrates the impact of improved accuracy in the calculations of these thermodynamic values. In some cases, substantial changes to these values may even expose flaws in current interpretations and motivate the development of a superior understanding of the concepts.

The implication of a slope greater than 1 for the $\Delta\text{BDE}(\text{M}-\text{C})$ versus $\Delta\text{BDE}(\text{C}-\text{H})$ correlation has significant consequences. In this scenario, the thermodynamic preference for C–H activation is to *generate the strongest metal–carbon bond* rather than to *break the weakest carbon–hydrogen bond* as might be expected. The formation of the stronger metal–carbon bond necessarily occurs at the expense of the stronger C–H bond in the starting material. This implies that reactions which occur by C–H oxidative addition are expected to have regioselectivities distinct from and orthogonal to radical abstraction reactions, where the weakest C–H bond reacts preferentially.

Experimentally determined bond energy correlations, while useful, are limited to cases where the metal complexes are well behaved and the reaction energetics are such that kinetic and equilibrium measurements can be reliably conducted using standard spectroscopic techniques. In many cases, reactions are too fast, have too few observables, or are sufficiently exergonic that direct experimental measurements are challenging to obtain. Computational chemistry has evolved such that highly accurate predictions and bond strengths and reaction energetics are reliable, provided that an appropriate quantum chemical model is applied and the results are interpreted correctly. For a useful guide on preventing common user errors and misconceptions in computational modeling of chemical reactions, a recent Tutorial by Baik and co-workers provides guidance.²¹

In the context of M–C versus H–C correlations, Eisenstein, Perutz, and co-workers calculated Rh–C and Ti–C versus C–H BDEs previously determined experimentally in the studies of Jones and Wolczanski.²² Employing density functional theory (DFT) calculations using two different functionals, these studies consistently reproduced the experimental bond energy correlations from the original publications.^{7,18,19} With the B3PWP91 functional, the slopes of the correlations were reproduced within 4% of the experimental values, slightly better agreement with the experimental results in comparison with that obtained when the BP86 functional was used (within 8%). The success of this computational bond energy correlation study demonstrates the utility of DFT in situations where experimental determinations of the desired bond

Scheme 2. Reaction of $(\eta^5\text{-C}_5\text{Me}_5)\text{Rh}(\text{PMe}_3)(\text{H})$ with *m*-Difluorobenzene to Generate Fluoroaryl Products by $\text{C}(\text{sp}^2)\text{-H}$ Oxidative Addition



strengths are not feasible. DFT studies may also be able to predict reactions with heightened affinity for metal–carbon bonding relative to carbon–hydrogen bonding, ostensibly a property that culminates in high regioselectivity in the activation of strong C–H bonds.

Over time, it has become apparent that the 1:1 correlations of M–C and C–H bond strengths obtained by Bryndza and Bercaw are exceptions rather than the rule. Siegbahn noted the importance of ionic contributions in transition-metal–carbon bonding,²³ and it is these ionic effects that typically render M–C bond strengths more sensitive to the identity of the organic fragment in comparison to that of the corresponding C–H bonds. Systems for which the correlation lies close to unity do so because of the electroneutrality principle;¹⁴ indeed, Bryndza and Bercaw observed a compensatory effect on the Ru–P bond strengths of $(\eta^5\text{-C}_5\text{Me}_5)\text{Ru}(\text{PMe}_3)\text{X}$ as the identity of X was varied.²⁴ Examples and implications of systems which deviate strongly from the 1:1 M–C/C–H correlation will be discussed in the next section.

The *ortho* Fluorine Effect: An Impactful Deviation.

While most early studies on M–C/C–H correlations primarily focused on metal–alkyl complexes, metal–aryl complexes can also exhibit interesting M–C/C–H bond correlations. In intermolecular chemistry, processes involving the oxidative addition of fluorinated arenes are demonstrative of how the thermodynamics of metal–carbon bond strengths may be leveraged for selective C–H oxidative addition and ultimately functionalization. A substantial amount of stoichiometric and catalytic chemistry has been reported that illustrates the effect of *ortho* fluorine substitution on M–C_{aryl} bond thermodynamics.²⁵

An early example of the “*ortho* fluorine effect” was reported by Jones, Perutz, and co-workers²⁶ with a cyclopentadienyl rhodium complex. Heating $(\eta^5\text{-C}_5\text{Me}_5)\text{Rh}(\text{PMe}_3)(\text{Ph})\text{H}$ resulted in elimination of benzene to generate the unsaturated rhodium(I) intermediate responsible for $\text{C}(\text{sp}^2)\text{-H}$ oxidative addition. In neat *m*-difluorobenzene at 67 °C over the course of 4 h, two isomeric rhodium(III) aryl hydride products were observed in a 5:1 ratio. The major product was $[\text{Rh}]-(2,4\text{-C}_6\text{H}_3\text{F}_2)$ with fluorine substituents *ortho* and *para* to the rhodium–carbon bond, while the minor product was the twice *meta*-substituted $[\text{Rh}]-(3,5\text{-C}_6\text{H}_3\text{F}_2)$ (Scheme 2). Under these conditions, none of the third possible isomer $[\text{Rh}]-(2,6\text{-C}_6\text{H}_3\text{F}_2)$ was detected. However, heating the solution to 78 °C for 20 h produced this product *exclusively*. These observations demonstrate that, while the formation of $[\text{Rh}]-(2,6\text{-C}_6\text{H}_3\text{F}_2)$ by $\text{C}(\text{sp}^2)\text{-H}$ oxidative addition is kinetically disfavored in comparison to the other rhodium(III) aryl hydride isomers, the thermodynamic product of the oxidative addition is the isomer with the greatest number of *ortho* fluorine substituents

to the M–C bond. The observed 5:1 ratio of kinetic products might appear significant, but statistics also contribute and likely dominate the outcome; there are two equivalent C–H bonds in the substrate whose activation gives the major kinetic product. It is useful in evaluating selectivities to acknowledge statistical differences.

Photochemical studies with the related rhodium ethylene complex $(\eta^5\text{-C}_5\text{Me}_5)\text{Rh}(\text{PMe}_3)(\text{C}_2\text{H}_4)$ were performed whereby irradiation promoted ethylene dissociation and formation of the rhodium intermediate active for C–H activation.²⁶ Experiments with various fluorinated arenes established a notable trend: *ortho* fluorine substituents impart thermodynamic stability to M–C bonds and determine which metal–aryl isomers are observed.

What is the origin of this preference? Subsequent DFT studies by Eisenstein and Perutz established that M–C(sp^2) bond strengths increase with increasing *ortho* to fluorine substitution, and this effect is general among metal–aryl complexes.²⁷ Calculation of the M–C and C–H bond dissociation free energies of series of metal–aryl complexes and the corresponding free arenes with zero, one, or two *ortho* fluorine substituents produced correlations with slopes (termed $R^{\text{MC/HC}}$ values) greater than 2.0 in most cases, indicating that the metal–carbon bonds in the complexes are more responsive to *ortho* fluorine substitution than the C–H bonds in the free arenes (Figure 6). It should be noted that *ortho* fluorine substituents also strengthen $\text{C}(\text{sp}^2)\text{-H}$ bonds in free aromatic compounds; however, the stabilization imparted to the corresponding M–C_{aryl} bond is greater in magnitude in comparison to that of the arene C–H bond.²⁷

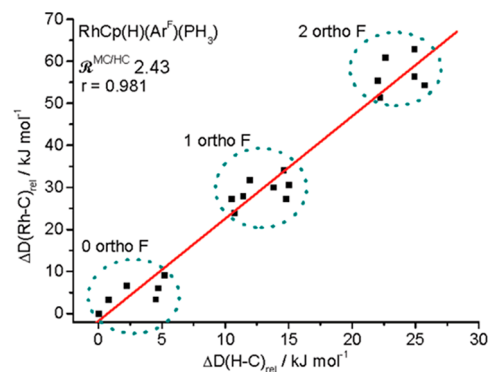


Figure 6. Plot of relative Rh–C BDEs of $(\eta^5\text{-C}_5\text{Me}_5)\text{Rh}(\text{H})(\text{Ar}^{\text{F}})(\text{PH}_3)$ vs the H–C BDEs in the corresponding fluorinated arenes. All relative BDE values were calculated using DFT and the B3PW91 functional. Reproduced with permission from ref 27. Copyright 2009 American Chemical Society.

Understanding *why* metal complexes magnify the *ortho* fluorine effect remains an active area of experimental and computational research and is an important frontier in organometallic chemistry. A commonly proposed rationale for the effect invokes the increased ionicity of the metal–carbon bond with increasing *ortho* fluorine substitution.^{3g,27} In the purely ionic limit, a metal cation is paired with an aryl anion and an inductively withdrawing fluorine substituent in the *ortho* position stabilizes the anionic component; more specifically, it is likely that the C–F σ^* antibonding orbital accepts electron density, stabilizing the bonding interaction (Figure 7). This explanation is consistent with the computa-

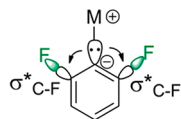
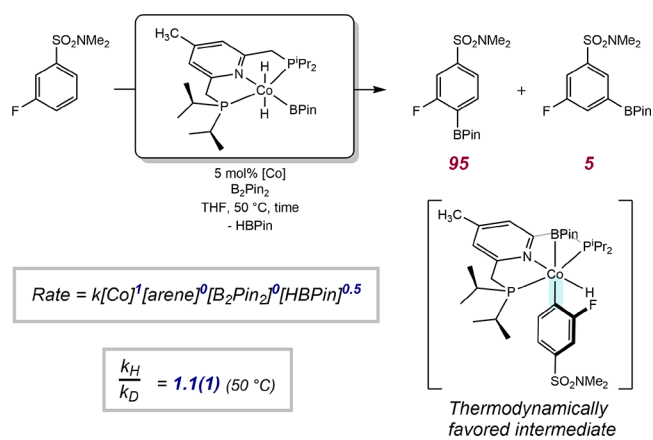


Figure 7. Representation of the stabilizing interaction that gives rise to the *ortho* fluorine effect: namely, negative hyperconjugation into the C–F σ^* orbital by the electrons in the M–C bond. Reproduced with permission from ref 3g. Copyright 2017 American Chemical Society.

tional findings of Eisenstein and Perutz, who found that complexes of first-row metals (i.e. those with more ionic metal–carbon bonding) generally exhibit greater calculated values of $R^{MC/HC}$ than do complexes of second- and third-row metals. Another possible explanation is that the carbons *ortho* to a fluorine substituent are stronger σ -donors as a result of the Pople–Gordon β -effect,²⁸ which has been used to rationalize the counterintuitive σ -donating ability of trifluoromethyl groups in both organic compounds and transition-metal–CF₃ complexes.²⁹ While the presence of a trifluoromethyl group makes an arene or complex more electron deficient *on the whole*, natural bond orbital analysis has demonstrated that *the individual atom* bonded to a trifluoromethyl group receives a significant partial negative charge; the same may very well be true of the carbon *ortho* to fluorine in a fluorinated arene.

Cobalt complexes of bis(phosphine)pyridine (ⁱP^rPNP) ligands promote the C(sp²)–H borylation of fluorinated arenes with high regioselectivity for the position *ortho* to the fluorine substituent.³⁰ This selectivity, which is improved over the statistical distribution of products observed with iridium/bipyridine catalysts, was initially attributed to the greater acidity of the *ortho* C–H bonds. A subsequent, comprehensive mechanistic investigation provided a more complete explanation for the origins of the observed regioselectivity.³¹ One notable finding was that the selectivity of the reaction was unaltered by reaction conditions such as temperature, choice of solvent, concentration, and order of addition. Kinetic analysis and deuterium kinetic isotope effect (KIE) studies support a mechanism whereby C(sp²)–H oxidative addition is fast and reversible. Due to the reversibility of C–H oxidative addition relative to subsequent steps, the thermodynamically favored *ortho* fluoroaryl intermediate is preferred, accounting for the observed *ortho* regioselectivity in the overall catalytic transformation (Scheme 3). Computational analysis analogous to that conducted by Eisenstein and Perutz established an $R^{MC/HC}$ value of 2.87, near the upper bound of the values obtained for this metric in previous studies.²⁷ This large value of $R^{MC/HC}$ indicates that not only is the *ortho* fluorine effect operative in [ⁱP^rPNP]Co-catalyzed borylation reactions but also these

Scheme 3. Regioselective, Cobalt-Catalyzed Borylation of Fluorinated Arenes at the Position *ortho* to the Fluorine Substituent and Experimental Data Supporting Reversible C(sp²)–H Oxidative Addition Favoring *o*-Fluoroaryl Intermediates

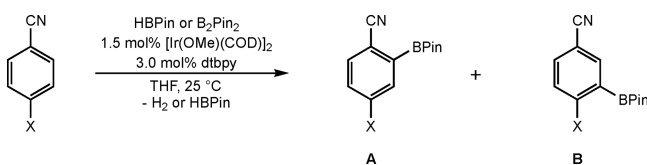


complexes are particularly sensitive to *ortho* fluorine substitution, contributing to the high observed selectivities.

■ KINETIC INFLUENCES ON REGIOSELECTIVITY

Influences of Sterics. The thermodynamic concepts applied above also imply that C–H activation processes should generally favor formation of the strongest possible metal–carbon bond. In practice, this is often not the case; instead, stoichiometric or catalytic reactions may occur with selectivities that are orthogonal to those anticipated from the thermodynamic heuristic. In one scenario, an *irreversible* C–H oxidative addition event results in kinetic control of regioselectivity. In such cases, steric effects often predominate in the determination of regioselectivity.

The iridium-catalyzed borylation of arenes is among the most widely applied and synthetically useful C–H functionalizations known, and it is a salient example of the role kinetic effects can play in regioselectivity outcomes. The groups of Smith and Hartwig independently introduced catalysts that borylate substituted arenes with reliable and predictable sterically driven site selectivity, favoring functionalization of spatially accessible positions.³² For example, the iridium-catalyzed borylation of selected 1,3-disubstituted arenes results exclusively in borylation of the 5-position to yield a substitution pattern that (depending upon the substituents in the starting material) can be challenging to achieve using electrophilic aromatic substitution chemistry.³³ A systematic study of the iridium-catalyzed borylation of 1,4-disubstituted arenes demonstrated that the reaction typically favored functionalization of the position *ortho* to the smaller of the two substituents.³⁴ A subset of these results examining selectivities with the 4-halonitriles provides a clear illustration of the trend (Table 1). Borylation of 4-fluorobenzonitrile proceeded with approximately 9:1 selectivity in favor of borylation *ortho* to the smaller fluorine substituent, but the regioselectivity inverts when fluorine is replaced by larger halogens. The preference for borylation *ortho* to the nitrile substituent improves to exclusivity in the reaction of 4-iodobenzonitrile, a result attributed to the increasing size of the halide substituent.

Table 1. Ir-Catalyzed C(sp²)-H Borylation of 4-Halobenzonitriles^a

entry	X	borane (equiv)	time (h)	yield (%)	A:B	steric enthalpy of X (kcal/mol)
1	F	HBPin (0.25)	8	71	11:89	1.535
2	Cl	HBPin (0.25)	36	76	80:20	4.133
3	Br	HBPin (0.25)	48	73	95:5	5.405
4	I	B ₂ Pin ₂ (1.0)	40	70	>99:1	7.759

^aSee ref 34 for primary data and definition of the steric enthalpy parameter. The reported steric enthalpy for the CN substituent is 3.211 kcal/mol.

Mechanistic studies on the catalytic borylation of arenes by iridium-bipyridine catalysts demonstrate a consistent mechanistic picture for all substrates examined thus far.³⁵ For benzene, *o*-dichlorobenzene, and 3-picoline, C(sp²)-H oxidative addition to an Ir(III)-boryl intermediate is turnover-limiting and irreversible; accordingly, the selectivity is determined by the difference in the activation energies for C-H oxidative addition at the various sites of the arene. That is to say, the regioselectivity in these reactions is under kinetic control, resulting in significant implications. The first is that the thermodynamics of forming the stronger metal-carbon bond are less relevant to the reaction selectivity; the reversibility of C-H oxidative addition is a necessary condition for the thermodynamics to predominate in determining the regioselectivity outcome. The second implication is that, for these kinetically controlled reactions, the barrier to oxidative addition should be significantly higher at sites *ortho* to sterically demanding substituents. This assertion has been supported computationally, as in the case of oxidative addition of toluene by an iridium tris(boryl) complex.³⁶ In this case, the reaction *ortho* to the methyl group was calculated to proceed with an activation barrier of 28.2 kcal/mol, in comparison to to 25.6 and 25.7 kcal/mol at the *meta* and *para* positions, respectively. The observed sterically derived regioselectivity is consistent with this concept; the *meta* and *para* products are those observed experimentally in the bipyridine/iridium-catalyzed borylation of toluene.^{32b}

Prediction of Regioselectivity When Multiple Positions Are Sterically Accessible. In cases where multiple arene C(sp²)-H bonds have comparable steric accessibility, prediction of the preferred site of functionalization is less straightforward. With steric factors being approximately equal, it is sensible to consider substrate electronic factors in the determination of selectivity. One of the most readily available and easily understood measures to compare the electronics of the available sites is C-H acidity. For this reason, it is tempting to use pK_a values to predict regioselectivity; however, this approach has limitations for C-H activations (or functionalizations) that occur by two-electron oxidative addition (*vide infra*). It should be noted that this strategy is generally more useful for reactions that occur by concerted metalation-deprotonation, a topic which will not be covered

in this Tutorial but which has been addressed in depth elsewhere.³⁷

The discussion of kinetic contributions to regioselectivity is continued with examples from iridium-catalyzed C(sp²)-H borylation, as these reactions are mechanistically well understood and much of the available data suggest that they are kinetically controlled. In one of the first studies that evaluated the acidity of C-H bonds as a predictive tool for the regioselectivity in iridium-catalyzed arene borylation,³⁸ Marder and co-workers explored three classes of model substrates, including monosubstituted and 1,2-disubstituted benzene derivatives as well as 2,7-disubstituted quinolines.³⁹ These substrate classes were selected to ensure that, in all cases, multiple sterically accessible but electronically differentiated sites were present in the substrate. The authors compared the experimental selectivity outcomes of borylation with the calculated C-H pK_a values for the positions borylated. While in most cases the more acidic position (of those which were sterically accessible) was borylated to a greater extent in comparison to the other sites, this trend was qualitative, as the magnitude of the pK_a difference did not reliably correlate to that of the observed selectivity. Moreover, there were some cases where the borylation of a less acidic C-H bond was favored.

It is worthwhile to recall that, by definition, pK_a is typically taken as a measure of thermodynamic acidity. It stands to reason that it would have limited predictive power for a reaction that is kinetically controlled and operates by concerted oxidative addition rather than by a heterolytic proton transfer pathway. Using pK_a as an indicator is appealing due to the relative ease of measurement or prediction by calculation; however, it appears that other metrics that are less readily obtained are superior predictors of site selectivity in iridium-catalyzed C(sp²)-H borylation. In a computational study, Merlic, Houk, and co-workers applied a distortion-interaction model to assess the origins of regioselectivity in these reactions.³⁶ Seventeen substrates for which the regioselectivity of Ir-catalyzed borylation was previously known were subject to this analysis; given the possible ramifications of the *ortho* fluorine effect in these reactions, it should be noted that no fluorinated arenes containing multiple distinct C(sp²)-H bonds in sterically unencumbered positions were included in the study. In a distortion-interaction model, the activation barrier for an intermolecular reaction is viewed as a combination of two components: the energy required to distort the ground-state reagents into the transition-state geometry and the energy associated with the interaction between the two distorted fragments (Figure 8). When such a model is applied, it is often the case that one component has more substantial effects upon the outcome of a reaction than the other or that the identity of the more significant component can change with the reaction conditions. In the case of iridium-catalyzed (hetero)arene borylation, Merlic and Houk found that the distortion energies were quite similar for the 17 substrates examined and did not correlate well with the experimentally observed regioselectivities. Instead, the interaction energies were found to be more dominant. Accordingly, the calculated BDEs of the Ir-C bond in the transition state correlated well with the activation energy and served as an effective predictor of the regioselectivity in borylation. Due to the lateness of the C-H oxidative addition transition state (and as a result of the Hammond postulate), the Ir-C BDEs in the resulting Ir-aryl intermediate predicted the regioselectiv-

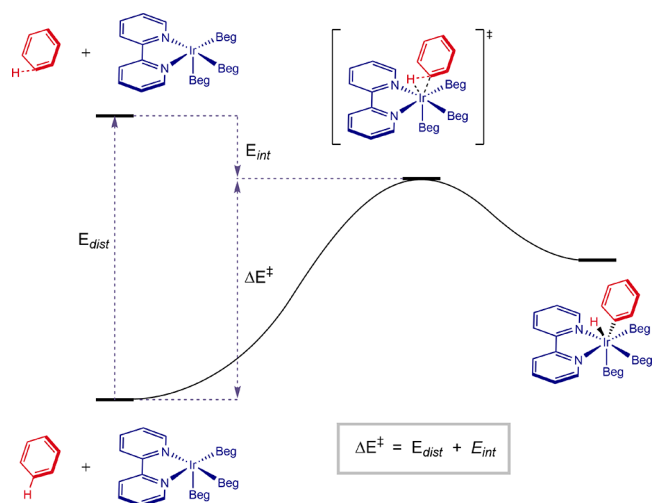


Figure 8. Schematic representation of the distortion–interaction analysis of the oxidative addition of benzene to (bpy)Ir(Beg)₃ (Beg = ethylene glycolatoboryl), representative of the turnover-limiting step in iridium-catalyzed C(sp²)–H borylation. Inspired by a Figure in ref 37a.

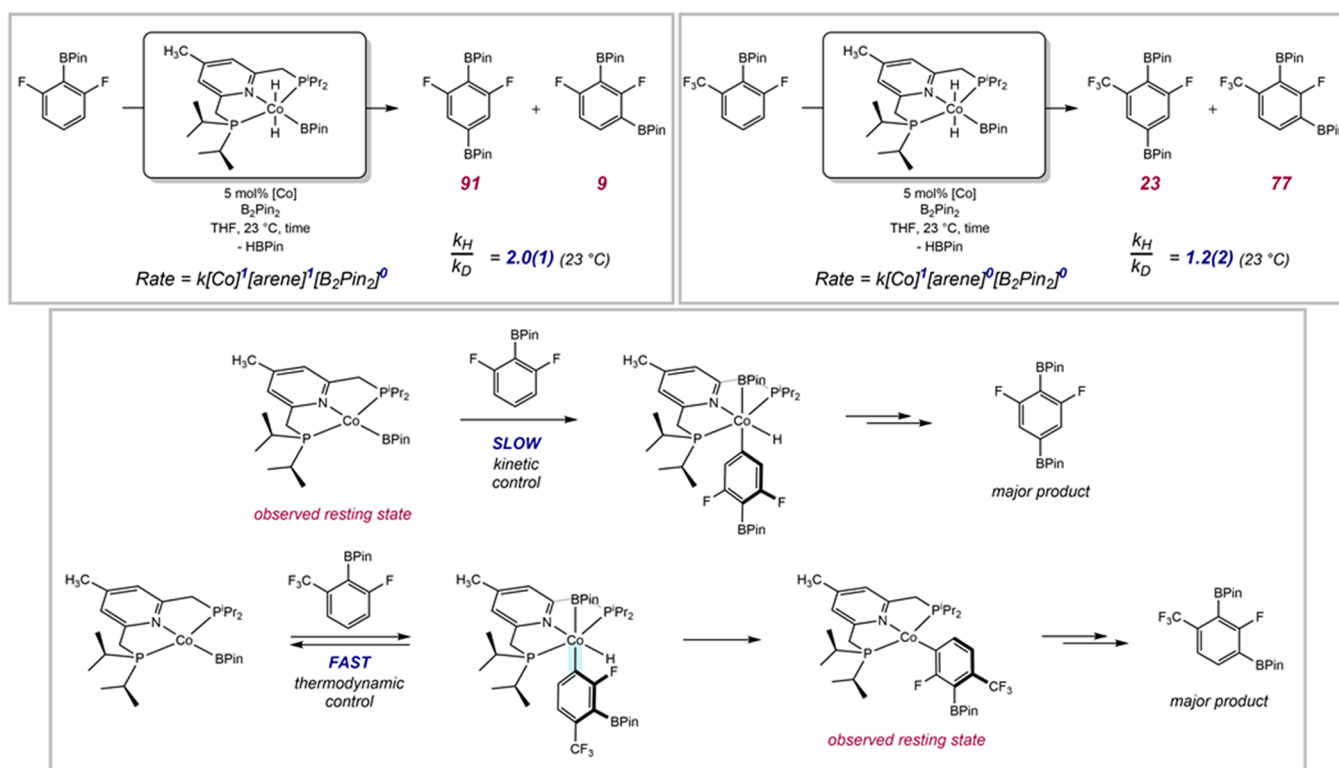
ities of the reactions with efficacy similar to that of the corresponding bond energy in the transition state.

Discrimination between Electronically Distinct C–H Sites in a Kinetically Controlled Reaction. In the examples of iridium-catalyzed C(sp²)–H borylation discussed above, it appears that kinetically controlled C(sp²)–H oxidative addition generally favors activation of more sterically accessible positions, with little deviations from statistical selectivity being observed in most cases. However, there have been some

reports where transition-metal catalysts effectively discriminate between electronically distinct C(sp²)–H sites in similar steric environments, resulting in selective functionalization.

Our laboratory has recently reported that cobalt complexes of ⁱPrPNP, which were previously shown to undergo regioselective borylation of fluorinated arenes at the position *ortho* to fluorine (vida supra),³⁰ can exhibit different electronically controlled selectivities depending on the substrate employed.⁴⁰ In the catalytic borylation of select arylboronate esters, a significant preference for borylation *para* to the initial boronate substituent was observed, and this selectivity overrides the previously established *ortho*-to-fluorine regioselectivity in substrates containing both boronate and fluorine substituents. Employing 2,6-difluorophenylboronic acid pinacol ester, which undergoes borylation with 91:9 regioselectivity favoring production of the *para*-diborylated product, as a representative substrate, the mechanism of this reaction was investigated using kinetics experiments, *in situ* spectroscopic studies, and kinetic isotope effect measurements (Scheme 4, top left). The combined results of these studies support a mechanism involving turnover-limiting C(sp²)–H oxidative addition of the arene substrate to a cobalt(I)–boryl resting state. Observation of the *para*-to-boronate product implies a kinetic preference for oxidative addition at the position *para* to the boronate substituent (Scheme 4, bottom). This may be rationalized in terms of the unique electronics of the boronate moiety, an inductive donor due to the greater electronegativity of carbon in comparison to boron.⁴¹ At the same time, the vacant p orbital of boron withdraws electron density from the arene ring through resonance effects. The combination of these inductive and resonance effects renders the position *para* to the boronate substituent as the most

Scheme 4. Catalytic *para*-to-Boronate (Top Left) and *ortho*-to-Fluorine (Top Right) Selective C(sp²)–H Borylation by Cobalt Precatalysts and Proposed Substrate-Dependent Selectivity-Determining Phenomena (Bottom)



electron deficient sterically accessible C(sp²)–H bond in the substrate, likely contributing to the more facile oxidative addition at this position in comparison to the adjacent sites. While it is tempting to attribute the observed kinetic regioselectivity to the apparent large size of the [BPin] substituent,⁴² borylation of an approximately isosteric acetal exhibited a 2:1 preference for borylation *para* to the acetal. While this result indicates that the size of the substituent has some influence on the regiochemical outcome of the catalytic reaction, it is clear that the electronics of the boronate substituent play an important role, resulting in the greater than 9:1 selectivity observed in the borylation of 2,6-difluorophenylboronic acid pinacol ester.

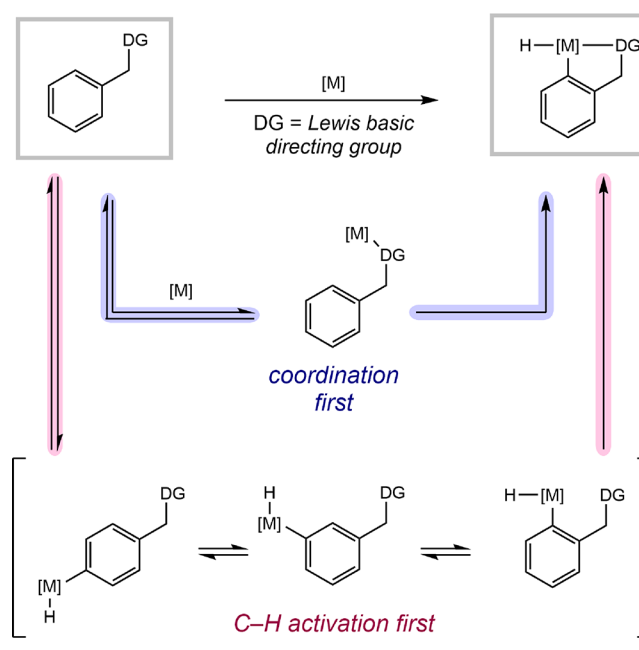
Notably, the borylation of fluorinated arenes with (iPr)³PNP Co catalysts exhibits a relationship between regioselectivity and mechanism that has not yet been rigorously investigated in the context of dtbpy/Ir-catalyzed C(sp²)–H borylation.⁴¹ When one of the fluorine substituents of 2,6-difluorophenylboronic acid pinacol ester was replaced with a more electron withdrawing trifluoromethyl substituent,⁴³ *ortho*-to-fluorine regioselectivity was observed (Scheme 4, top right). Mechanistic investigations established that this inversion of regioselectivity was accompanied by changes in the relative rates of the fundamental steps of the catalytic cycle; no dependence on the concentration of the arene substrate was observed, and KIE experiments provided a value near unity, indicating that the use of a more electron deficient substrate accelerated C(sp²)–H oxidative addition to the extent that thermodynamic (rather than kinetic) control of C(sp²)–H oxidative addition was restored (Scheme 4, bottom). This rare example wherein regioselectivity changes dramatically due to differing electronic properties of the substrates employed may further enable unique and useful regioselectivities in C(sp²)–H functionalization.

■ CHELATE-DIRECTED C–H BOND CLEAVAGE

Chelate Effects and Possible Mechanisms. In both stoichiometric and catalytic processes for the cleavage of C(sp²)–H bonds, chelation is often used as a strategy to impart *ortho* selectivity. Conceptually, a functional group on the substrate that is typically a Lewis base serves as a ligand for the metal to direct the *ortho* C–H bond for oxidative addition. Following Murai's innovative use of this strategy in Ru-catalyzed alkene hydroarylation,⁴⁴ this concept has been developed extensively and widely applied to the regioselective activation and functionalization of C–H bonds.⁵ Since Murai's seminal report, most strategies relying on chelation have been applied to *ortho*-selective reactions. However, these concepts have been extended using thoughtfully designed catalyst–substrate interactions to affect more challenging regioselectivities: for example, *meta* to the directing group.⁴⁵

To further understand the principles underlying the regioselectivity arising from chelate assistance, two limiting possibilities are presented. In the most frequently invoked scenario, the directing group coordinates to the transition metal, and it is the resulting metal–substrate complex that undergoes the C(sp²)–H activation event (Scheme 5, inner pathway). In another scenario, the C(sp²)–H activation step occurs indiscriminately but reversibly at several sites on the substrate before coordination of the directing group preferentially traps one of the C(sp²)–H activation products (Scheme 5, outer pathway). The distinction between the two mechanisms is not only of fundamental and pedagogical

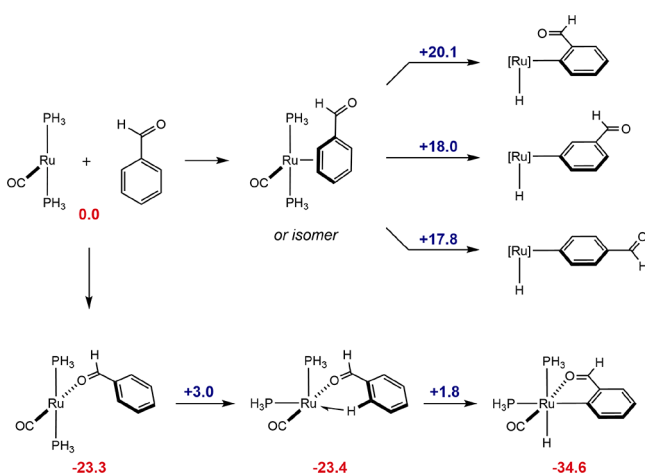
Scheme 5. Two Limiting Pathways for Chelate-Assisted *ortho*-C–H Activation



importance, it also can have implications for the design of regioselective reactions. However, definitive support for or, more rigorously, elimination of one pathway over the other is rare. The reason for this is straightforward—in most cases it is extremely difficult to experimentally distinguish the operative pathway. However, in some cases, insights into the role of chelate effects have been obtained from computations or experiments from the careful interrogation of particularly cooperative systems.

The mechanism that involves initial coordination of the directing group to the metal is commonly invoked in regioselective C–H activation and functionalization reactions, sometimes in the absence of supporting experimental evidence. In catalytic applications, this premise relies on the supposition that the coordination of the directing group to the transition metal lowers the activation barrier for the C–H bond-breaking process in comparison to the analogous reaction without chelate assistance. If this were not the case, the substrate might readily undergo C–H activation without the need for directing group coordination; without participation of the directing group, the desired selectivity would not be observed.

The Murai reaction, reported in 1993, is often cited as one of the pioneering examples of directed C–H functionalization.⁴⁴ It is important to note that the authors in their landmark publication suggested that a mechanism involving initial directing-group participation was operative but also conceded that the exact sequence of events was "not yet clear". A subsequent computational investigation evaluated the energetics of the olefination of benzaldehyde and provided compelling support for Murai's proposal (Scheme 6).⁴⁶ At the B3LYP level of theory, the most energetically favorable pathway involves initial coordination of the carbonyl oxygen atom and subsequent formation of an agostic aryl C–H, which then undergoes C(sp²)–H oxidative addition at the *ortho* position to generate the discrete ruthenium–aryl–hydride intermediate. Subsequent olefin insertion and C–C reductive elimination furnish the observed hydroarylation product. Notably, the barrier to C–H oxidative addition was calculated

Scheme 6. Calculated C–H Oxidative Addition Pathways for the Murai Reaction^a

^aRed values under intermediates indicate calculated ground-state energies relative to $\text{Ru}(\text{PH}_3)_2(\text{CO})$ and PhCHO , and blue values over reaction arrows provide the calculated activation barriers relative to the previous intermediate. All values are reported in kcal/mol.

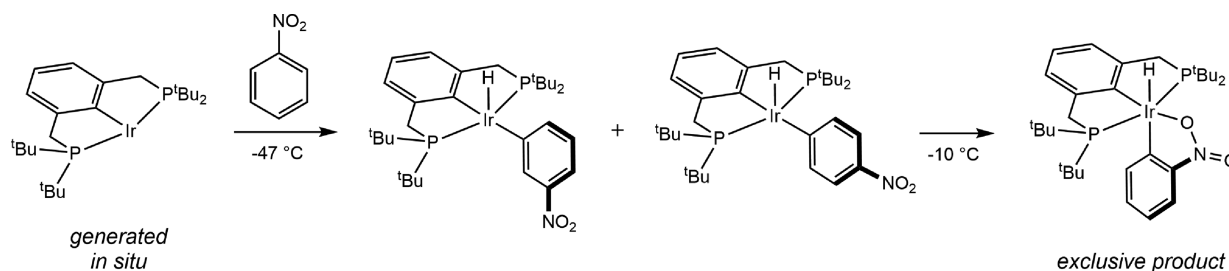
to be just 1.8 kcal/mol. The low barrier step was compared to analogous steps in pathways lacking precoordination of the oxygen atom. If instead, for example η^2 -coordination of the π -system of the arene to the metal occurs prior to C–H oxidative addition, activation of the *ortho* position proceeds with a much higher calculated activation barrier of 20.1 kcal/mol. Not only is this pathway more energetically demanding than that involving carbonyl oxygen coordination prior to C–H oxidative addition but it would also fail to explain the observed *ortho* regioselectivity, as reactions of the *meta* and *para* C–H bonds were calculated to have lower barriers of 18.0 and 17.8 kcal/mol, respectively. An energetic difference of 2.0 kcal/mol between two reactions corresponds to a more than 10-fold difference in reaction rate, assuming the concentrations of reactants are equal. That the *meta* and *para* oxidative addition products would be kinetically preferred in the absence of chelate effects is consistent with the kinetic preference of oxidative addition discussed previously in the context of iridium-catalyzed arene borylation (*vide supra*). Lacking coordination of the directing group to the metal, this substituent serves as a blocking group, raising the barrier to C–H oxidative addition at the *ortho* positions.

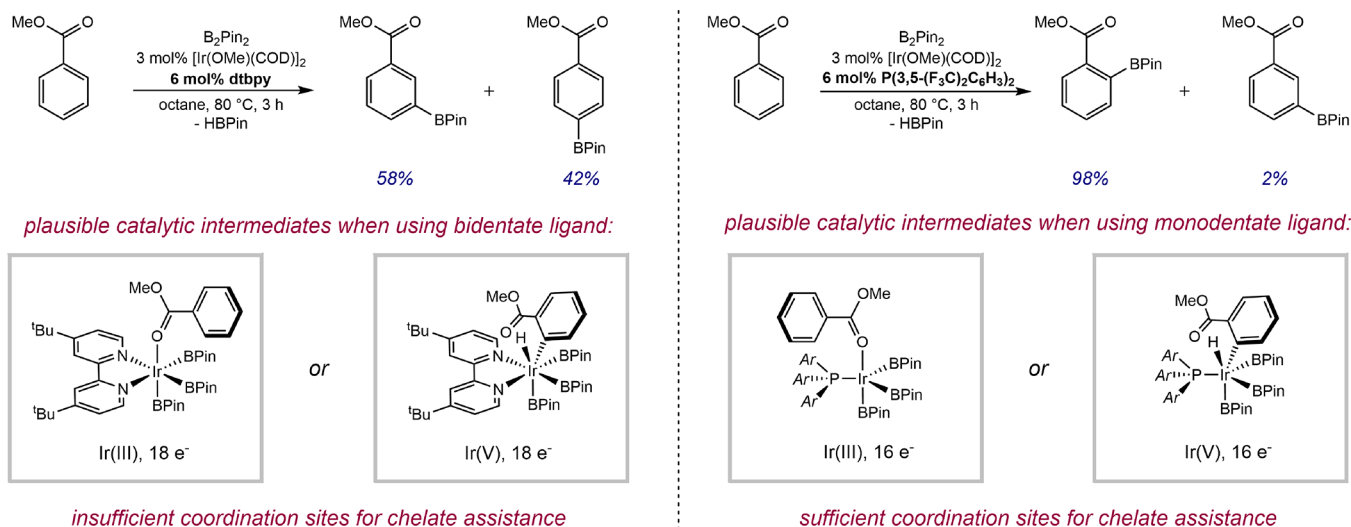
Although the Murai-inspired mechanism of chelation-assisted C–H activation is much more commonly proposed than other possible mechanisms, it is important to note that it is not always the case that coordination of the directing group

occurs prior to the C–H activation step. Goldman and co-workers reported compelling experimental evidence that, in the case of a $[(\text{PCP})\text{Ir}]$ complex, C–H activation of nitrobenzene or acetophenone likely occurs by a mechanism involving C(sp^2)–H oxidative addition prior to the coordination of the directing group (Scheme 7).⁴⁷ An *in situ* NMR analysis revealed that oxidative addition of all the arene C–H bonds occurs reversibly and, in fact, kinetically favors the more sterically accessible sites *meta* and *para* to the directing group, consistent with the examples discussed up to this point. However, subsequent coordination of the functional group (either nitro or acetyl) generates a thermodynamically stabilized chelate that traps the product of *ortho* C–H activation. The overall result is exclusive selectivity for the *ortho* position over the *meta* and *para* positions. Characterization of the oxidative addition product by single-crystal X-ray diffraction revealed a complex with mutually *trans* hydride and aryl ligands. This arrangement of ligands offers additional experimental evidence for a mechanism that terminates with coordination of the directing group, as chelate-directed C–H oxidative addition would be expected to produce a complex with the aryl and hydride ligands *cis* to one another.

Prerequisite for an Available Coordination Site. A common requirement of any mechanism involving *ortho*-directed C–H bond activation is the availability of an additional open coordination site. In the case of the “coordination-first” mechanism, metal complexes with one fewer available coordination site than those needed for both directing-group coordination and C–H oxidative addition would either undergo (a) ligand coordination without subsequent productive C–H activation or (b) undirected, kinetically controlled C–H oxidative addition at the most sterically accessible sites. A possible “C–H cleavage-first” mechanism would be unable to trap the *ortho* product by intramolecular coordination of the directing group.

To illustrate the necessity of an open coordination site for chelate-directed C–H activation, iridium-catalyzed arene borylation is again pedagogically informative, where drastically different regioselectivity outcomes have been obtained by adjusting the ligand denticity. Ishiyama, Miyaura, and co-workers noted that borylation of methyl benzoate using B_2Pin_2 with an iridium–bipyridine catalyst provided high turnover numbers but none of the *ortho*-borylated product was observed despite the presence of the ester, which one might expect to act as an *ortho*-directing group.⁴⁸ Instead, a 58:42 ratio of the *meta*- and *para*-borylated products was obtained. The identity of the C–H activating species offers insight into the observed regioselectivity; a 16-electron (bipyridine) $\text{Ir}(\text{BPin})_3$ complex has only one available coordination site, and this complex

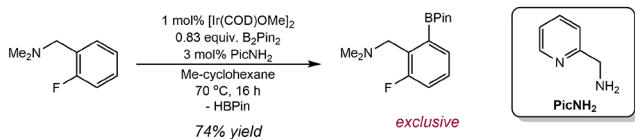
Scheme 7. Selective *o*-C(sp^2)–H Oxidative Addition of Nitrobenzene That Occurs by Trapping of the Kinetically Disfavored *ortho*-Activated Intermediate by the Chelating Nitro Group

Scheme 8. Effects of Ligand Denticity in Iridium-Catalyzed C(sp²)-H Borylation of Arenes with Pendant Lewis Basic Groups

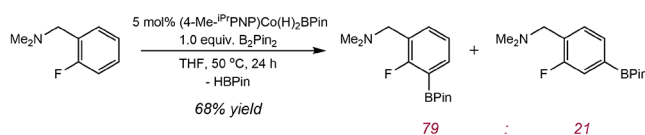
cannot exploit chelate effects to afford *ortho*-selective borylation (Scheme 8, left). Exchanging the bidentate bipyridine ligand for a monodentate phosphine ostensibly opens a coordination site and enables a pathway that allows for both coordination of the ester to the metal and C(sp²)-H oxidative addition. Under the optimized conditions, selectivities of 98:2 in favor of the *ortho*-borylated product were observed (Scheme 8, right). In a follow-up computational investigation, Jover and Maseras provided support for this explanation.⁴⁹ Use of a monodentate phosphine enables initial coordination of the ester, which is then followed by chelate-assisted *ortho* C-H oxidative addition, giving rise to the observed regioselectivity.

In some cases, the availability of metal coordination sites enables synthetically useful, orthogonal regioselectivities in catalytic C-H activation and functionalization. In Ir-catalyzed C(sp²)-H borylation, the replacement of the standard bipyridine ligand with a hemilabile ligand such as 2-picolyamine produced regioselective borylation of the position *ortho* to a pendant benzylic tertiary amine (Scheme 9a).⁵⁰ The observation of this selectivity suggests that, at some point in the catalytic cycle, 2-picolyamine serves as a monodentate ligand to allow coordination of the substrate directing group

and chelate-assisted C-H oxidative addition. In contrast, the (PNP)Co catalysts developed in our laboratory “ignore” the directing group and instead maintain *ortho*-to-fluorine regioselectivity in the borylation of a substrate containing either fluorine or benzylic tertiary amine substituents (Scheme 9b).³⁰ The indifference of the (PNP)Co catalysts toward a Lewis basic directing group results from the lack of ample coordination sites to facilitate chelate assistance; the C-H activating cobalt-boryl intermediate is a 16-electron, square-planar derivative, and coordination of the directing group to generate a coordinatively saturated 18-electron intermediate is unproductive. Without productive substrate chelation, *ortho*-to-fluorine regioselectivity is observed as a result of the thermodynamic *ortho* fluorine effect.

Scheme 9. Catalytic C(sp²)-H Borylation of a Benzylic Tertiary Amine Using (a) a Hemilabile Ir Catalyst for Which Substrate Chelation Directs C-H Oxidative Addition and (b) a (PNP)Co Catalyst That Does Not Participate in Substrate Chelation(a) Iridium/PicNH₂: Chelation-Assisted

(b) Cobalt/PNP: No Chelate Assistance

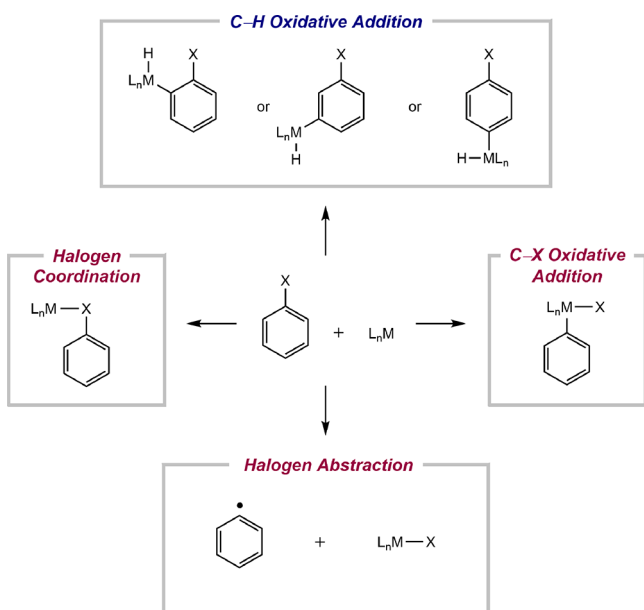


CHEMOSELECTIVITY OF OXIDATIVE ADDITION

Relevance of Aryl Halides. Aryl halides are an important class of molecules in organic chemistry due to their synthetic versatility, particularly as electrophiles in cross-coupling reactions.⁵¹ Successful transformations of these substrates using C(sp²)-H functionalization methods result in products that can then be further modified by exploiting the reactivity of the halide substituent. A combination of challenges and opportunities are presented when methods for the functionalization of C(sp²)-H (or C-X, where X is a halogen) bonds in aryl halides are considered (Scheme 10). For example, the presence of a halide substituent changes the chemical properties of the various C-H bonds of the arene; whether sterics or electronics at each site is more significant in determining regioselectivity tends to be a characteristic of the particular transition-metal complex involved. It is also possible for the halide substituent to act as a directing group in some cases.⁵² In other scenarios, the chemoselectivity of oxidative addition of a metal complex may favor reaction at C-X bonds rather than C-H bonds, as is the case in Pd-catalyzed cross-coupling reactions.^{51,53} In yet another possibility, halogen atom abstraction may outcompete all oxidative addition pathways.⁵⁴

An interesting question in chemoselectivity therefore arises—when is C-H versus C-X oxidative addition favored and why? In the former case, what is the impact on regioselectivity? In the latter, what determines the rate of oxidative addition in a substrate with multiple halogens? There are catalysts known

Scheme 10. Selected Generic Reactions of Aryl Halides and Transition Metals



that promote the selective oxidative addition of $C(sp^2)-H$ bonds in the presence of $C(sp^2)-X$. Many of these are underappreciated, and a rationalization of this selectivity and prospects for additional catalyst development will be part of our focus. Systematic studies of $C-X$ versus $M-X$ bond energy relationships analogous to those for $C-H$ bonds such as those reported by Bryndza and Bercaw,¹⁰ Anderson and Bergman,¹⁶ Jones,^{7,18} and Wolczanski^{9,17} would be desirable for guiding such an analysis but are scarce in the literature. This is principally due to the paucity of well-behaved complexes and reactions that are required to perform such an experimental thermochemical study.⁵⁵ In lieu of these correlation studies, relevant experimental and computational results from the chemical literature will be discussed that offer insight into the determination of chemo- and regioselectivity in oxidative additions of aryl halides.

C-H Activation vs C-F Activation. Before the reactivity of aryl halides in oxidative addition reactions is presented, the fundamental chemical properties of these molecules warrant discussion. The experimental $C-H$ and $C-X$ BDEs of benzene and the aryl halides are reported in Table 2.⁵⁶ With a BDE of 112.9 kcal/mol, the $C-H$ bonds in benzene are stronger than all of the $C-H$ and $C-X$ bonds in the aryl halides with the

Table 2. Bond Dissociation Energies of Benzene and Aryl Halides^a

X	BDE (kcal/mol)
H	112.9 ± 1.5
F	125.6 ± 2.0
Cl	95.5 ± 1.5
Br	80.4 ± 1.5
I	65.0 ± 1.0

^aValues are taken from ref 56.

exception of the $C-F$ bond in fluorobenzene, which has an experimental BDE of 125.6 kcal/mol. As is well-known in organic chemistry and from periodic trends, descending the halogen series results in weaker $C(sp^2)-X$ bonds, with the $C-I$ bond in iodobenzene at 65.0 kcal/mol. On the basis of bond strengths, it is remarkable when metal complexes promote $C(sp^2)-F$ oxidative addition preferentially to $C(sp^2)-H$ activation.⁵⁷

The origins of the preference for $C(sp^2)-H$ oxidative addition in the reaction of 1,4-difluorobenzene with $Os(CO)(PH_3)_2$ was explored computationally by Eisenstein, Perutz, and Caulton.⁵⁸ At the time, it was unknown whether the product of $C-H$ or $C-F$ oxidative addition would be thermodynamically favored. Of the six possible isomeric products, the product arising from $C-F$ oxidative addition where the fluoride ligand was in the basal plane and the aryl group was in the apical position (Basal F, Figure 9) was found to be the most stable by a substantial 16.2 kcal/mol. The $C-H$ oxidative addition product was the next most stable isomer, where the hydride is in the apical position. The stability of the various products is dependent not only on the chemoselectivity

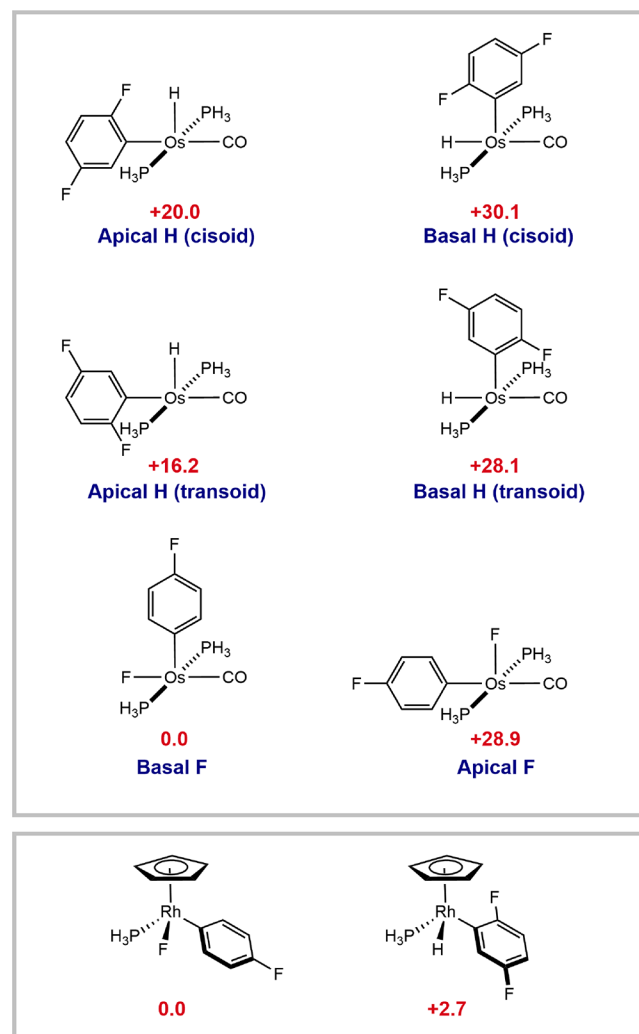


Figure 9. DFT calculated (B3LYP functional) energies of the possible oxidative addition products of *p*-difluorobenzene with (top) $Os(CO)(PH_3)_2$ and (bottom) $(\eta^5-C_5H_5)Rh(PH_3)$. All values are given in kcal/mol.

of the oxidative addition but also on a balance of the π -donating properties of the fluoride and the π -back-bonding of the carbonyl ligands. The competing effects resulted in a situation described by the authors as “a case where the traditionally defined bond dissociation energy may be of little use for determining reaction thermodynamics”. To minimize these complications, a similar analysis was conducted with the more conformationally rigid complex $(\eta^5\text{-C}_5\text{H}_5)\text{Rh}(\text{PH}_3)$. This compound was selected for further computational study by analogy to $(\eta^5\text{-C}_5\text{H}_5)\text{Rh}(\text{PMe}_3)$, which is known to selectively cleave the $\text{C}(\text{sp}^2)\text{-H}$ bonds of fluorinated arenes.²⁶ With $(\eta^5\text{-C}_5\text{H}_5)\text{Rh}(\text{PH}_3)$, the isomer arising from C-F oxidative addition of *p*-difluorobenzene was more stable than that arising from reaction of the C-H bond by 2.7 kcal/mol.

According to computations, oxidative addition of the $\text{C}(\text{sp}^2)\text{-F}$ bond to $(\eta^5\text{-C}_5\text{H}_5)\text{Rh}(\text{PH}_3)$ is thermodynamically preferred over reaction with the $\text{C}(\text{sp}^2)\text{-H}$ bond. However, the $\text{C}(\text{sp}^2)\text{-H}$ product is observed experimentally from the reaction of fluorinated arenes with $(\eta^5\text{-C}_5\text{H}_5)\text{Rh}(\text{PMe}_3)$, implying a kinetic preference for $\text{C}(\text{sp}^2)\text{-H}$ activation. The transition-state energies for both oxidative addition reactions were computed from a common rhodium arene complex starting point, $(\eta^5\text{-C}_5\text{H}_5)\text{Rh}(\text{PH}_3)(\eta^2\text{-1,4-C}_6\text{F}_2\text{H}_4)$.⁵⁹ The transition state leading to C-H oxidative addition was 9.4 kcal/mol higher in energy than this intermediate, while the barrier for C-F activation was found to be 33.3 kcal/mol (Figure 10). This disparity of 23.9 kcal/mol accounts for the

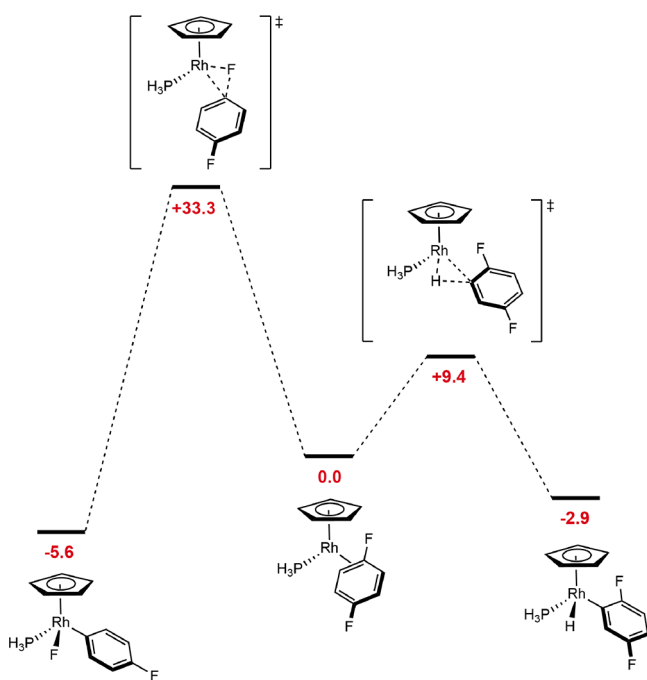


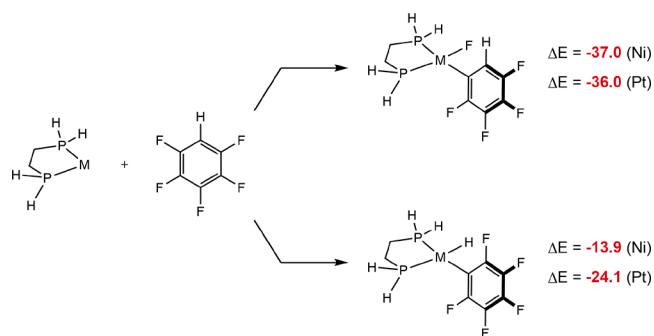
Figure 10. Calculated reaction coordinate diagram for (left) $\text{C}(\text{sp}^2)\text{-F}$ (left) and $\text{C}(\text{sp}^2)\text{-H}$ (right) oxidative addition starting from $\text{CpRh}(\text{PH}_3)(\eta^2\text{-C}_6\text{F}_2\text{H}_4)$. All values are given in kcal/mol.

experimentally observed C-H chemoselectivity. Inspection of the C-H oxidative addition transition structure reveals highly synchronous Rh-C and Rh-H bond formation concomitant with C-H bond breaking. In contrast, the transition structure required for C-F oxidative addition features a concerted asynchronous process where C-F bond cleavage and Rh-F bond formation are substantial while Rh-C bond formation

lags behind. It appears that the destabilizing effect of C-H bond cleavage is compensated by the interaction energy of the forming Rh-C and Rh-H bonds in the C-H activation transition state, while the lack of stabilizing Rh-C bond formation in the C-F transition state is the origin for the much higher barrier to this process.

While the reactivity differences among first-, second-, and third-row metals are understood in general terms, direct comparisons of homologous complexes between metals in the same group are as insightful as they are rare. One example relating to the chemoselectivity of the oxidative addition of fluoroarenes will be presented. Stone and co-workers observed that $(\text{PCy}_3)_2\text{Pt}$ undergoes selective C-H oxidative addition with pentafluorobenzene to generate *trans*- $(\text{PCy}_3)_2\text{Pt}(\text{C}_6\text{F}_5)\text{-H}$.⁶⁰ In a later report, Perutz and co-workers established that the same reaction with the nickel congener $(\text{PEt}_3)_2\text{Ni}$ proceeded by oxidative addition at the various C-F bonds rather than the aryl C-H bond.⁶¹ A theoretical study by McGrady and Perutz sought to rationalize the difference in chemoselectivity between first- and third-row transition metal congeners.⁶² Using the model complexes $\text{M}(\text{H}_2\text{PCH}_2\text{CH}_2\text{PH}_2)$ ($\text{M} = \text{Ni}$ and Pt) and pentafluorobenzene as a representative substrate, the pathways to C-H and C-F (at the position *ortho* to the lone C-H bond in the substrate) oxidative addition were calculated by DFT and compared (Scheme 11). All four processes are exothermic, and the

Scheme 11. Calculated Thermochemistry for the $\text{C}(\text{sp}^2)\text{-F}$ (Top) or $\text{C}(\text{sp}^2)\text{-H}$ Oxidative Addition (Bottom) of Pentafluorobenzene to $\text{M}(\text{PH}_2\text{CH}_2\text{CH}_2\text{PH}_2)$ ($\text{M} = \text{Ni}, \text{Pt}$)^a



^aAll values are given in kcal/mol.

differences in exothermicity offer insight into the preference for C-F activation with nickel and C-H activation with platinum. Notably, for either metal, the reaction of the C-F bond was the more exothermic transformation. The C-F oxidative addition reaction was found to be similarly exergonic with Ni (-37.0 kcal/mol) and Pt (-36.0 kcal/mol), while C-H oxidative addition was more downhill with Pt (-24.1 kcal/mol) than with Ni (-13.9 kcal/mol); these computational data suggest that the disparate chemoselectivities are kinetic rather than thermodynamic. Transition-state calculations support a higher barrier for C-F oxidative addition for Pt than for Ni, which is attributed to the repulsive $(5d)\pi\text{-}p\pi$ interactions in the transition state; an analysis of the transition structures reveals that the Pt-C and Pt-F bonds are formed to a lesser extent in comparison to the corresponding bonds in the Ni case, supporting this explanation.

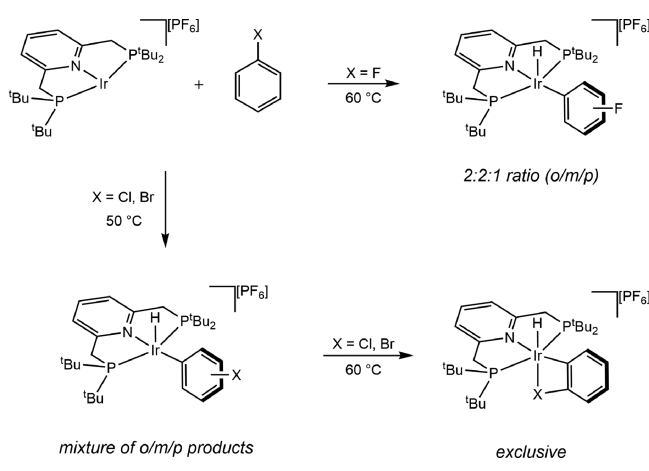
Upon a survey of the literature and consideration of the complexes that have been shown to selectively cleave C-F

bonds, electron-rich complexes of Ni and early metals such as W exhibit unique performance.⁶³ The efficacy of both classes of compounds is consistent with the deleterious effects of $d\pi$ – $p\pi$ repulsion. The Ni complexes are sufficiently electron rich to cleave the strong C–F bond, while their 3d orbitals are less diffuse than those of a second- or third-row metal, lessening $d\pi$ – $p\pi$ repulsion despite the high electron count of the d^{10} metal. In the case of earlier metals, lower d-electron counts enable C–F cleavage even with second- or third-row metal complexes. Harmon and co-workers have shown that, in the case of a TpW complex, the intermediacy of a discrete F-bound σ -complex can enable lower energy pathways to C–F oxidative addition, resulting in selective activation in the presence of aryl C–H bonds.⁶⁴

C–H Activation vs C–Cl, –Br, and –I Activation. The oxidative addition of aryl–chloride, –bromide, or –iodide is a crucial step in the metal-catalyzed cross-coupling reactions that have become ubiquitous in medicinal and synthetic organic chemistry. The impact and importance of these reactions was recognized with the 2010 Nobel Prize in Chemistry to Heck, Negishi, and Suzuki.⁵¹ While these reactions, often involving Pd, selectively result in coupling at the aryl halide linkage despite the (typical) presence of $C(sp^2)$ –H bonds in the molecule, this chemoselectivity is not conserved among all transition metals. For example, the iridium borylation catalysts previously discussed catalyze chemoselective $C(sp^2)$ –H borylation even in the presence of more polar carbon–halogen bonds.^{32–35} These discrepancies will be addressed along with some general predictive principles for chemoselectivity in the oxidative addition of aryl halides.

In a stoichiometric study on the oxidative addition of aryl halides to a cationic bis(phosphine)pyridine iridium(I) complex, Milstein and co-workers demonstrated selective $C(sp^2)$ –H oxidative addition in the presence of $C(sp^2)$ –F, $C(sp^2)$ –Cl, and $C(sp^2)$ –Br bonds (Scheme 12).⁵² The

Scheme 12. Reaction of a Cationic (PNP)Ir Complex with (Top) Fluorobenzene and (Bottom) Chloro- or Bromobenzene



reaction of fluorobenzene proceeded with statistical regioselectivity for the possible C–H activation products (a 2:2:1 ratio of the *ortho*, *meta*, and *para* products). Upon reaction with chlorobenzene or bromobenzene, all regioisomeric products resulting from C–H oxidative addition are initially observed. At increased reaction times, the various isomers convert entirely to the *ortho*-activated product. A solid-state

structure of the major product of reaction of chlorobenzene established chloride coordination to the metal. These data, reminiscent of the prior study by Goldman⁴⁷ on C–H oxidative addition of nitrobenzene to an iridium pincer complex, support a mechanism involving kinetically competitive C–H activation at all positions of the arene followed by subsequent trapping of the *ortho*-activated product by chelation of the halide substituent.

An experimental study by Ozerov and co-workers provided unique and powerful insights into the kinetic and thermodynamic oxidative addition preferences of a neutral iridium complex.⁶⁵ Addition of chlorobenzene at room temperature produced a mixture of four C–H oxidative addition products, ostensibly including *ortho*-, *meta*-, and *para*-activated products with two rotamers of either the *ortho* or *meta* product (Scheme 13). A small (5%) amount of the C–Cl oxidative addition product was also detected under these conditions. Raising the temperature of the reaction mixture to 70 °C for 72 h resulted in slow isomerization of the multiple C–H oxidative addition products to a thermodynamically preferred *ortho*-activated product. The amount of C–Cl activation product was unchanged under these conditions. Continued thermolysis of the mixture above 100 °C resulted in primarily the C–Cl oxidative addition product. This progression of product distributions thoroughly establishes the energetics of oxidative addition for this system. The initial observation of various C–H activation products indicates that these are all kinetically accessible products, while the minor C–Cl activation product arises from a more kinetically demanding process. That equilibration at increased temperatures favors the production of an *ortho*-activated product implies a thermodynamic preference for this product over the other isomers resulting from C–H oxidative addition. While one might suspect that chelation of the chloride ligand is responsible for this apparent kinetic preference, a solid-state structure of the complex reveals no such coordination; instead, it may be that the inductively withdrawing *ortho* chloride substituent stabilizes the metal–aryl bond in analogy to the well-established *ortho* fluorine effect. Finally, the preferential production of the C–Cl oxidative addition product at still higher temperatures suggests that this is the thermodynamically favored product of the reaction, which is kinetically inaccessible at the lower temperatures. Similar behavior was observed in the oxidative addition of bromobenzene, indicating that the kinetic and thermodynamic preferences of oxidative addition are similar for both halogens. Overall, this work provided compelling evidence that C–H oxidative addition is the kinetically favored process, while thermodynamically preferred C–X oxidative addition may be observed at higher temperatures.

In subsequent experimental investigations of the oxidative addition of aryl halides, Ozerov and co-workers found that (PNP)Rh complexes analogous to the iridium complexes used in previous studies selectively activated carbon–halogen bonds with no observation of C–H oxidative addition products.⁶⁶ As was noted previously, such direct comparisons between transition metals of the same group are rare and instructive, and further insights on these topics often require computational studies. To advance the fundamental understanding of the different chemoselectivities observed with second- and third-row metals, Wu and Hall published theoretical investigations on truncated (for computational expedience) versions of both the (PNP)Ir⁶⁷ and (PNP)Rh⁶⁸ complexes (Figure 11). Both studies specifically investigated the C–H or

Scheme 13. Kinetic C(sp²)-H Oxidative Addition and Thermodynamic C(sp²)-Cl Oxidative Addition from a Neutral (PNP)Ir^I Complex

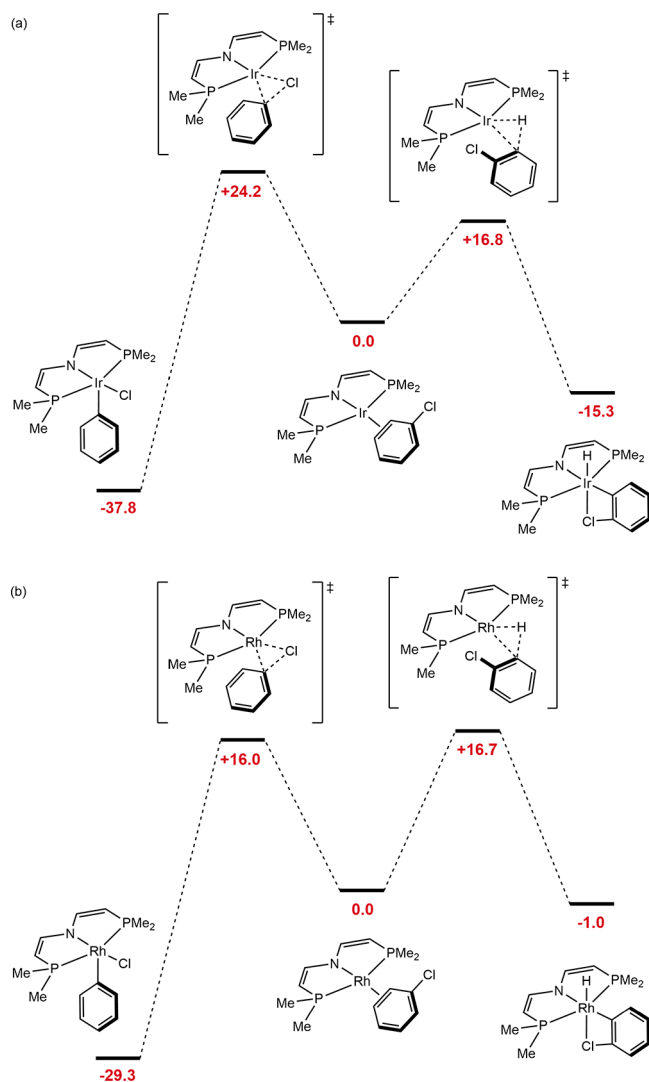
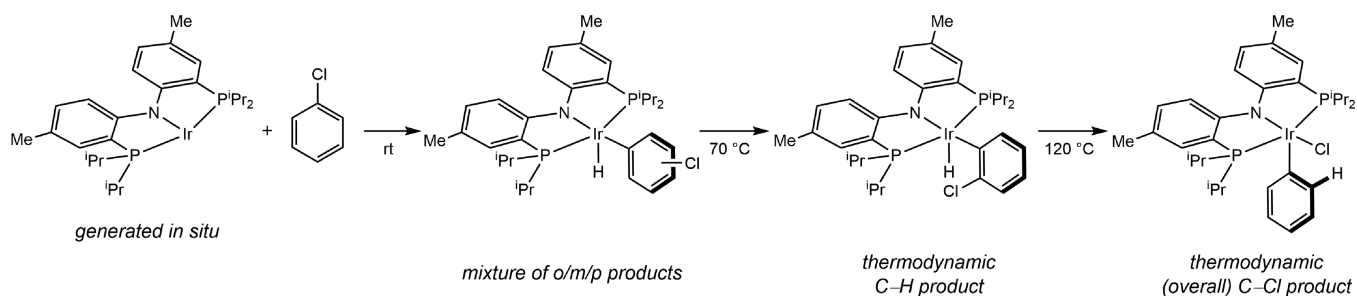


Figure 11. Calculated reaction coordinate diagrams for competitive C(sp²)-Cl and C(sp²)-H oxidative addition of chlorobenzene with neutral PNP complexes of (top) Ir and (bottom) Rh. All values are given in kcal/mol. Note that the value of 0.0 is equal to the energy of the arene π -complex and is different for the Rh and Ir coordinates.

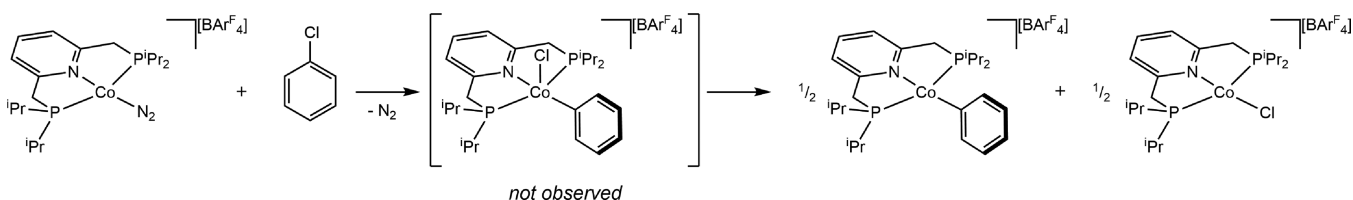
C-Cl oxidative additions of chlorobenzene. For the iridium example, C-H oxidative addition at the position *ortho* to the chlorine substituent was kinetically favored over C-Cl oxidative addition by 7.0 kcal/mol, consistent with the experimental kinetic preference for C-H activation at relatively low temperatures; however, the C-Cl oxidative

addition product was favored thermodynamically over the major C-H activation product by a substantial 22.6 kcal/mol. In the Rh system, C-Cl oxidative addition was still found to be thermodynamically favored over C-H oxidative addition; in this case the products differed in energy by 28.3 kcal/mol. Activation barriers en route to C-H and C-Cl oxidative addition were reported to be similar, within 0.7 kcal/mol. The observation of selective C-Cl activation in the Ozerov study is therefore more likely due to the reversibility of C-H activation, as any C-H oxidative addition product formed can funnel irreversibly to the thermodynamically favored C-Cl oxidative addition product.

Of the four reactions depicted in Figure 11, the C-Cl oxidative addition to the Ir pincer complex represents an energetic outlier, with an activation barrier 7–8 kcal/mol higher than those of the other three oxidative additions. This apparent anomaly has been addressed by Wolczanski and co-workers and speaks to the reactivity differences between second- and third-row transition metals.⁶⁹ Relativistic contraction of the 6s orbitals and expansion of the 5d orbitals result in significant mixing, rendering the d_{z²} orbital of the (PNP)Ir complex less nucleophilic than that of the corresponding Rh complex. The presence of lone pair electrons on the chloride substituent renders the oxidative addition of C-Cl more challenging than that of C-H, which can be easily activated by either Rh or Ir.

A general trend for the chemoselectivity of oxidative addition arises whereby third-row metals prefer activation of C-H bonds and lighter congeners prefer C-X oxidative addition. Cationic (PNP)Co complexes⁷⁰ analogous to the iridium system⁵² investigated by Milstein provide pedagogical insights. Recall that the iridium examples exhibited high selectivity for C-H oxidative addition with aryl halides. Using the cationic Co complex with essentially the same pincer ligand, addition of chloro- or bromobenzene produced no detectable C(sp²)-H activation products. Instead, a 1:1 mixture of (PNP)CoX (X = Cl, Br) and (PNP)CoPh was observed, a result consistent with initial C-X oxidative addition followed by comproportionation (Scheme 14). Notably, this chemoselectivity observed in stoichiometric reactions of the cationic iridium and cobalt complexes is of consequence to the neutral borylation catalysts based upon each metal. In iridium-catalyzed C(sp²)-H borylation, halogen substituents (other than fluoride) act as steric blocking groups that prevent C-H oxidative addition at the *ortho* positions.⁵² In contrast, cobalt-catalyzed C(sp²)-H borylation is incompatible with these substrates because the rate of C-X (X = Cl, Br, I) oxidative addition exceeds that of C-H oxidative addition.²⁹

Scheme 14. Reaction of a Pincer Cobalt Complex with Chlorobenzene by Two-Electron $C(sp^2)$ -Cl Oxidative Addition Followed by Comproportionation to Generate Equal Amounts of Phenyl and Chloride Complexes



Halogen atom transfer pathways are also plausible with first-row transition-metal complexes. Budzelaar and co-workers observed that oxidative addition of alkyl and aryl halides with pyridine(diimine) cobalt dinitrogen complexes occurred by initial halogen atom abstraction followed by reaction of the resulting organoradical species with another equivalent of the Co complex.⁵⁴ Distinguishing reactions that occur by this mechanism from those that proceed by two-electron oxidative addition followed by comproportionation may be difficult; however, the halogen atom abstraction pathway generates unequal mixtures of the metal-halide and metal-aryl products due to the occurrence of side reactions of the organic radical intermediate, whereas the two-electron oxidative addition mechanism is expected to produce a 1:1 ratio of products.

The presence of halogens on an arene substrate offers new possibilities for the chemo- and regioselectivity of $C(sp^2)$ -H or $C(sp^2)$ -X oxidative addition, and it is beneficial to consider the general reactivity trends that can be gleaned from the literature. First, it is apparent that C-X oxidative addition is thermodynamically favored in comparison to C-H oxidative addition for X = any halogen. Thus, whether activation of C-H or C-X occurs preferentially is a kinetic phenomenon. In the case of late, third-row transition metals, C-H oxidative addition is the kinetically favored process and occurs preferentially; it is possible that this is a result of $d\pi$ - $p\pi$ repulsion between filled metal d orbitals and the lone pair (or filled π^* orbital) of the carbon-halogen bond, as has been proposed in the context of sluggish C-F activation in platinum complexes.⁶² The propensity for C-X oxidative addition increases as a group is ascended (and valence shell d orbitals contract), which seems to be consistent with this hypothesis. Moreover, 6s-5d mixing can render third-row transition metals less nucleophilic than their second-row counterparts, which can raise the activation barrier to C-X oxidative activation.⁶⁹ Lower barriers to C-X activation relative to C-H activation among first- and second-row metals manifest in a greater prevalence of the thermodynamically favored process.^{67,68} In the first row, the reactivity of the C-X bond outpaces C-H oxidative addition, and processes involving halogen atom abstraction have the capacity to complicate reactions involving the former.⁵⁴

CONCLUSIONS

The ubiquity of C-H bonds in organic molecules gives rise, simultaneously, to the great potential and the intrinsic challenge associated with C-H functionalization. Even relatively “simple” compounds contain numerous C-H bonds that differ, if only slightly, in their steric environments and electronic properties. The opportunities in synthesis and catalysis appear limitless if methods can be realized that effectively distinguish between these available sites. Gaining mechanistic insights and understanding the energetic principles

that govern the preference for reactivity at a given site are tantamount to realizing these goals. In addition, it is remarkable that, even after extensive studies into C-H oxidative addition over the past four decades, much remains to be learned to understand the reactivity in substituted substrates. Organometallic compounds continue to take center stage in these efforts, with rational ligand design remaining a central theme. While considerable progress has been made, C-H functionalization has yet to reach its full potential in synthesis, and pursuits in understanding and achieving predictable site selectivity are ongoing.

AUTHOR INFORMATION

Corresponding Author

Paul J. Chirik – Department of Chemistry, Princeton University, Princeton, New Jersey 08544, United States; orcid.org/0000-0001-8473-2898; Email: pchirik@princeton.edu

Author

Tyler P. Pabst – Department of Chemistry, Princeton University, Princeton, New Jersey 08544, United States; orcid.org/0000-0003-4595-2833

Complete contact information is available at: <https://pubs.acs.org/10.1021/acs.organomet.1c00030>

Notes

The authors declare no competing financial interest.

ACKNOWLEDGMENTS

The authors wish to thank Professor Peter T. Wolczanski (Cornell University) and Paul O. Peterson for helpful discussions. Financial support was provided by the NIH (SR01GM121441). T.P.P. thanks Amgen for financial support and Princeton University for an Edward C. Taylor Fellowship.

REFERENCES

- Arndtsen, B. A.; Bergman, R. G.; Mobley, T. A.; Peterson, T. H. Selective Intermolecular Carbon-Hydrogen Bond Activation by Synthetic Metal Complexes in Homogeneous Solution. *Acc. Chem. Res.* **1995**, *28*, 154–162.
- Labinger, J. A.; Bercaw, J. E. Understanding and exploiting C-H bond activation. *Nature* **2002**, *417*, 507–514.
- (a) Labinger, J. A. Platinum-Catalyzed C-H Functionalization. *Chem. Rev.* **2017**, *117*, 8483–8496. (b) Schwach, P.; Pan, X.; Bao, X. Direct Conversion of Methane to Value-Added Chemicals over Heterogeneous Catalysts: Challenges and Prospects. *Chem. Rev.* **2017**, *117*, 8497–8520. (c) Gunsalus, N. J.; Koppaka, A.; Park, S. H.; Bischof, S. M.; Hashiguchi, B. G.; Periana, R. A. Homogeneous Functionalization of Methane. *Chem. Rev.* **2017**, *117*, 8521–8573. (d) Wang, V. C.-C.; Maji, S.; Chen, P. P.-Y.; Lee, H. K.; Yu, S. S.-F.; Chan, S. I. Alkane Oxidation: Methane Monooxygenases, Related Enzymes, and Their Biomimetics. *Chem. Rev.* **2017**, *117*, 8574–8621. (e) Xue, X.-S.; Ji, P.; Zhou, B.; Cheng, J.-P. The Essential Role of

- Bond Energetics in C–H Activation/Functionalization. *Chem. Rev.* **2017**, *117*, 8622–8648. (f) Davies, D. L.; Macgregor, S. A.; McMullin, C. L. Computational Studies of Carboxylate-Assisted C–H Activation and Functionalization at Group 8–10 Transition Metal Centers. *Chem. Rev.* **2017**, *117*, 8649–8709. (g) Eisenstein, O.; Milani, J.; Perutz, R. N. Selectivity of C–H Activation and Competition between C–H and C–F Bond Activation at Fluorocarbons. *Chem. Rev.* **2017**, *117*, 8710–8753. (h) He, J.; Wasa, M.; Chan, K. S. L.; Shao, Q.; Yu, J.-Q. Palladium-Catalyzed Transformations of Alkyl C–H Bonds. *Chem. Rev.* **2017**, *117*, 8754–8786. (i) Yang, Y.; Lan, J.; You, J. Oxidative C–H/C–H Coupling Reactions between Two (Hetero)arenes. *Chem. Rev.* **2017**, *117*, 8787–8863. (j) Wei, Y.; Hu, P.; Zhang, M.; Su, W. Metal-Catalyzed Decarboxylative C–H Functionalization. *Chem. Rev.* **2017**, *117*, 8864–8907. (k) Newton, C. G.; Wang, S.-G.; Oliveira, C. C.; Cramer, N. Catalytic Enantioselective Transformations Involving C–H Bond Cleavage by Transition-Metal Complexes. *Chem. Rev.* **2017**, *117*, 8908–8976. (l) Kim, D.-S.; Park, W.-J.; Jun, C.-H. Metal–Organic Cooperative Catalysis in C–H and C–C Bond Activation. *Chem. Rev.* **2017**, *117*, 8977–9015. (m) Yi, H.; Zhang, G.; Wang, H.; Huang, Z.; Wang, J.; Singh, A. K.; Lei, A. Recent Advances in Radical C–H Activation/Radical Cross-Coupling. *Chem. Rev.* **2017**, *117*, 9016–9085. (n) Shang, R.; Ilić, L.; Nakamura, E. Iron-Catalyzed C–H Bond Activation. *Chem. Rev.* **2017**, *117*, 9086–9139. (o) Collins, T. J.; Ryabov, A. D. Targeting of High-Valent Iron-TAML Activators at Hydrocarbons and Beyond. *Chem. Rev.* **2017**, *117*, 9140–9162. (p) Hummel, J. R.; Boerth, J. A.; Ellman, J. A. Transition-Metal-Catalyzed C–H Bond Addition to Carbonyls, Imines, and Related Polarized π Bonds. *Chem. Rev.* **2017**, *117*, 9163–9227. (q) Crabtree, R. H. Homogeneous Transition Metal Catalysis of Acceptorless Dehydrogenative Alcohol Oxidation: Applications in Hydrogen Storage and to Heterocycle Synthesis. *Chem. Rev.* **2017**, *117*, 9228–9246. (r) Park, Y.; Kim, Y.; Chang, S. Transition Metal-Catalyzed C–H Amination: Scope, Mechanism, and Applications. *Chem. Rev.* **2017**, *117*, 9247–9301. (s) Murakami, K.; Yamada, S.; Kaneda, T.; Itami, K. C–H Functionalization of Azines. *Chem. Rev.* **2017**, *117*, 9302–9332. (t) Dong, Z.; Ren, Z.; Thompson, S. J.; Xu, Y.; Dong, G. Transition-Metal-Catalyzed C–H Alkylation Using Alkenes. *Chem. Rev.* **2017**, *117*, 9333–9403. (u) Fumagalli, G.; Stanton, S.; Bower, J. F. Recent Methodologies That Exploit C–C Single-Bond Cleavage of Strained Ring Systems by Transition Metal Complexes. *Chem. Rev.* **2017**, *117*, 9404–9432. (v) Qin, Y.; Zhu, L.; Luo, S. Organocatalysis in Inert C–H Bond Functionalization. *Chem. Rev.* **2017**, *117*, 9433–9520.
- (4) Cernak, T.; Dykstra, K. D.; Tyagarajan, S.; Vachal, P.; Krska, S. W. The medicinal chemist's toolbox for late stage functionalization of drug-like molecules. *Chem. Soc. Rev.* **2016**, *45*, 546–576.
- (5) Meng, G.; Lam, N. Y. S.; Lucas, E. L.; Saint-Denis, T. G.; Verma, P.; Cheksin, N.; Yu, J.-Q. Achieving Site-Selectivity for C–H Activation Processes Based on Distance and Geometry: A Carpenter's Approach. *J. Am. Chem. Soc.* **2020**, *142*, 10571–10591.
- (6) Chirik, P. J. Editorial: Introducing Tutorials. *Organometallics* **2015**, *34*, 4783.
- (7) Wick, D. D.; Jones, W. D. Energetics of Homogeneous Intermolecular Vinyl and Allyl Carbon-Hydrogen Bond Activation by the 16-Electron Coordinatively Unsaturated Organometallic Fragment [Tp'Rh(CNCH₂CM₂)]. *Organometallics* **1999**, *18*, 495–505.
- (8) (a) Mader, E. A.; Davidson, E. R.; Mayer, J. M. Large Ground-State Entropy Changes for Hydrogen Atom Transfer Reactions of Iron Complexes. *J. Am. Chem. Soc.* **2007**, *129*, 5153–5166. (b) Mader, E. A.; Manner, V. W.; Markle, T. F.; Wu, A.; Franz, J. A.; Mayer, J. M. Trends in Ground-State Entropies for Transition Metal Based Hydrogen Atom Transfer Reactions. *J. Am. Chem. Soc.* **2009**, *131*, 4335–4345.
- (9) Wolczanski, P. T. Activation of Carbon–Hydrogen Bonds via 1,2-RH-Addition-Elimination to Early Transition Metal Imides. *Organometallics* **2018**, *37*, 505–516.
- (10) Bryndza, H. E.; Fond, L. K.; Paciella, R. A.; Tam, W.; Bercaw, J. E. Relative Metal-Hydrogen, -Oxygen, -Nitrogen, and -Carbon Bond Strengths for Organoruthenium and Organoplatinum Compounds; Equilibrium Studies of Cp*(PMe₃)₂RuX and (DPPE)MePtX Systems. *J. Am. Chem. Soc.* **1987**, *109*, 1444–1456.
- (11) Bryndza, H. E.; Tam, W. Monomeric Metal Hydroxides, Alkoxides, and Amides of the Late Transition Metals: Synthesis, Reactions, and Thermochemistry. *Chem. Rev.* **1988**, *88*, 1163–1188.
- (12) Schilling, J. B.; Goddard, W. A.; Beauchamp, J. L. Theoretical Studies of Transition-Metal Methyl Ions, MCH₃⁺ (M = Sc, Cr, Mn, Zn, Y, Mo, Tc, Pd, Cd). *J. Am. Chem. Soc.* **1987**, *109*, 5573–5580.
- (13) Labinger, J. A.; Bercaw, J. E. Metal–Hydride and Metal–Alkyl Bond Strengths: The Influence of Electronegativity Differences. *Organometallics* **1988**, *7*, 926–928.
- (14) Pauling, L. The Nature of the Chemical Bond. Application of Results Obtained from the Quantum Mechanics and from a Theory of Paramagnetic Susceptibility to the Structure of Molecules. *J. Am. Chem. Soc.* **1931**, *53*, 1367–1400.
- (15) Bennett, J. L.; Vaid, T. P.; Wolczanski, P. T. Extracting absolute titanium-alkyl and hydride bond enthalpies from relative D(TiR(H)) in (silox)₂(tBu₃SiNH)TiR: electronegativity and ECT models. *Inorg. Chim. Acta* **1998**, *270*, 414–423.
- (16) Holland, P. L.; Anderson, R. A.; Bergman, R. G.; Huang, J.; Nolan, S. P. Monomeric Cyclopentadienylnickel Methoxo and Amido Complexes: Synthesis, Characterization, Reactivity, and Use for Exploring the Relationship between H–X and M–X Bond Energies. *J. Am. Chem. Soc.* **1997**, *119*, 12800–12814.
- (17) Tilset, M.; Parker, V. D. Solution Homolytic Bond Dissociation Energies of Organotransition-Metal Hydrides. *J. Am. Chem. Soc.* **1989**, *111*, 6711–6717.
- (18) Jones, W. D.; Hessell, E. T. Photolysis of Tp'Rh(CN-neopentyl)(η^2 -PhN=C=N-neopentyl) in Alkanes and Arenes: Kinetic and Thermodynamic Selectivity of [Tp'Rh(CN-neopentyl)] for Various Types of C–H Bonds. *J. Am. Chem. Soc.* **1993**, *115*, 554–562.
- (19) (a) Bennett, J. L.; Wolczanski, P. T. Energetics of C–H Bond Activation and Ethylene Binding to d⁰ Transient (silox)₂Ti = NSi^tBu₃. *J. Am. Chem. Soc.* **1994**, *116*, 2179–2180. (b) Bennett, J. L.; Wolczanski, P. T. Selectivities in Hydrocarbon Activation: Kinetic and Thermodynamic Investigations of Reversible 1,2-RH-Elimination from (silox)₂(^tBu₃SiNH)TiR (silox = ^tBu₃SiO). *J. Am. Chem. Soc.* **1997**, *119*, 10696–10719.
- (20) Jones, W. D.; Feher, F. J. The Mechanism and Thermodynamics of Alkane and Arene Carbon–Hydrogen Bond Activation in (C₅Me₅)Rh(PMe₃)(R)H. *J. Am. Chem. Soc.* **1984**, *106*, 1650–1663.
- (21) Ryu, H.; Park, J.; Kim, H. K.; Park, J. Y.; Kim, S.-T.; Baik, M.-H. Pitfalls in Computational Modeling of Chemical Reactions and How To Avoid Them. *Organometallics* **2018**, *37*, 3228–3239.
- (22) Clot, E.; Mégret, C.; Eisenstein, O.; Perutz, R. N. Validation of the M–C/H–C Bond Enthalpy Relationship through Application of Density Functional Theory. *J. Am. Chem. Soc.* **2006**, *128*, 8350–8357.
- (23) Siegbahn, P. E. M. Trends of Metal–Carbon Bond Strengths in Transition Metal Complexes. *J. Phys. Chem.* **1995**, *99*, 12723–12729.
- (24) Bryndza, H. E.; Domaille, P. J.; Tam, W.; Fong, L. K.; Paciello, R. A.; Bercaw, J. E. Comparison of Metal–Hydrogen, –Oxygen, –Nitrogen and –Carbon Bond Strengths and Evaluation of Functional Group Additivity Principles for Organoruthenium and Organoplatinum Compounds. *Polyhedron* **1988**, *7*, 1441–1452.
- (25) An early work in which selective oxidative addition of a fluorinated arene was observed: Tolman, C. A.; Ittel, S. D.; English, A. D.; Jesson, J. P. Chemistry of 2-Naphthyl Bis[bis(dimethylphosphino)ethane] Hydride Complexes of Iron, Ruthenium, and Osmium. 3. Cleavage of sp² C–H bonds. *J. Am. Chem. Soc.* **1979**, *101*, 1742–1751.
- (26) Selmeczy, A. D.; Jones, W. D.; Partridge, M. G.; Perutz, R. N. Selectivity in the Activation of Fluorinated Aromatic Hydrocarbons by [(C₅H₅)Rh(PMe₃)₃] and [(C₅Me₅)Rh(PMe₃)₃]. *Organometallics* **1994**, *13*, 522–532.
- (27) Clot, E.; Mégret, C.; Eisenstein, O.; Perutz, R. N. Exceptional Sensitivity of Metal–Aryl Bond Energies to ortho-Fluorine Substituents: Influence of the Metal, the Coordination Sphere, and the

Spectator Ligands on M-C/H-C Bond Energy Correlations. *J. Am. Chem. Soc.* **2009**, *131*, 7817–7827.

(28) Pople, J. A.; Gordon, M. Molecular Orbital Theory of the Electronic Structure of Organic Compounds. I. Substituent Effects and Dipole Moments. *J. Am. Chem. Soc.* **1967**, *89*, 4253–4261.

(29) (a) Tomashenko, O. A.; Grushin, V. V. Aromatic Trifluoromethylation with Metal Complexes. *Chem. Rev.* **2011**, *111*, 4475–4521. (b) Algarra, A. G.; Grushin, V. V.; Macgregor, S. A. Natural Bond Orbital Analysis of the Electronic Structure of $[\text{LnM}(\text{CH}_3)]$ and $[\text{LnM}(\text{CF}_3)]$ Complexes. *Organometallics* **2012**, *31*, 1467–1476.

(30) Obligacion, J. V.; Bezdek, M. J.; Chirik, P. J. $\text{C}(\text{sp}^2)$ -H Borylation of Fluorinated Arenes Using an Air-Stable Cobalt Precatalyst: Electronically Enhanced Site Selectivity Enables Synthetic Opportunities. *J. Am. Chem. Soc.* **2017**, *139*, 2825–2832.

(31) Pabst, T. P.; Obligacion, J. V.; Rochette, E.; Pappas, I.; Chirik, P. J. Cobalt-Catalyzed Borylation of Fluorinated Arenes: Thermodynamic Control of $\text{C}(\text{sp}^2)$ -H Oxidative Addition Results in *ortho*-to-Fluorine Selectivity. *J. Am. Chem. Soc.* **2019**, *141*, 15378–15389.

(32) (a) Cho, J.-Y.; Tse, M. K.; Holmes, D.; Maleczka, R. E.; Smith, M. R. Remarkably Selective Iridium Catalysts for the Elaboration of Aromatic C–H Bonds. *Science* **2002**, *295*, 305–308. (b) Ishiyama, T.; Takagi, J.; Ishida, K.; Miyaura, N.; Anastasi, N. R.; Hartwig, J. F. Mild Iridium-Catalyzed Borylation of Arenes. High Turnover Numbers, Room Temperature Reactions, and Isolation of a Potential Intermediate. *J. Am. Chem. Soc.* **2002**, *124*, 390–391.

(33) Murphy, J. M.; Liao, X.; Hartwig, J. F. Meta Halogenation of 1,3-Disubstituted Arenes via Iridium-Catalyzed Arene Borylation. *J. Am. Chem. Soc.* **2007**, *129*, 15434–15435.

(34) Chotana, G.; Rak, M. A.; Smith, M. R. Sterically Directed Functionalization of Aromatic C–H Bonds: Selective Borylation Ortho to Cyano Groups in Arenes and Heterocycles. *J. Am. Chem. Soc.* **2005**, *127*, 10539–10544.

(35) (a) Boller, T. M.; Murphy, J. M.; Hapke, M.; Ishiyama, T.; Miyaura, N.; Hartwig, J. F. Mechanism of the Mild Functionalization of Arenes by Diboron Reagents Catalyzed by Iridium Complexes. Intermediacy and Chemistry of Bipyridine-Ligated Iridium Trisboryl Complexes. *J. Am. Chem. Soc.* **2005**, *127*, 14263–14278. (b) Larsen, M. A.; Hartwig, J. F. Iridium-Catalyzed C–H Borylation of Heteroarenes: Scope, Regioselectivity, Application to Late-Stage Functionalization, and Mechanism. *J. Am. Chem. Soc.* **2014**, *136*, 4287–4299.

(36) Green, A. G.; Liu, P.; Merlic, C. A.; Houk, K. N. Distortion/Interaction Analysis Reveals the Origins of Selectivities in Iridium-Catalyzed C–H Borylation of Substituted Arenes and 5-Membered Heterocycles. *J. Am. Chem. Soc.* **2014**, *136*, 4575–4583.

(37) (a) Lafrance, M.; Rowley, C. N.; Woo, T. K.; Fagnou, K. Catalytic Intermolecular Direct Arylation of Perfluorobenzenes. *J. Am. Chem. Soc.* **2006**, *128*, 8754–8756. (b) Gorelsky, S. I.; Lapointe, D.; Fagnou, K. Analysis of the Concerted Metalation-Deprotonation Mechanism in Palladium-Catalyzed Direct Arylation Across a Broad Range of Aromatic Substrates. *J. Am. Chem. Soc.* **2008**, *130*, 10848–10849. (c) Gorelsky, S. I.; Lapointe, D.; Fagnou, K. Analysis of the Palladium-Catalyzed (Aromatic)C–H Bond Metalation–Deprotonation Mechanism Spanning the Entire Spectrum of Arenes. *J. Org. Chem.* **2012**, *77*, 658–668. (d) Wang, L.; Carrow, B. P. Oligothiophene Synthesis by a General C–H Activation Mechanism: Electrophilic Concerted Metalation–Deprotonation (eCMD). *ACS Catal.* **2019**, *9*, 6821–6836.

(38) For an earlier report on relationships between C–H acidity and borylation selectivity, see: Vanchura, B. A.; Preshlock, S. M.; Roosen, P. C.; Kallepalli, V. A.; Staples, R. J.; Maleczka, R. E.; Singleton, D. A.; Smith, M. R. Electronic effects in iridium C–H borylations: insights from unencumbered substrates and variation of boryl ligand substituents. *Chem. Commun.* **2010**, *46*, 7724–7726.

(39) Tajuddin, H.; Harrisson, P.; Bitterlich, B.; Collings, J. C.; Sim, N.; Batsanov, A. S.; Cheung, M. S.; Kawamorita, S.; Maxwell, A. C.; Shukla, L.; Morris, J.; Lin, Z.; Marder, T. B.; Steel, P. G. Iridium-catalyzed C–H borylation of quinolines and unsymmetrical 1,2-

disubstituted benzenes: insights into steric and electronic effects on selectivity. *Chem. Sci.* **2012**, *3*, 3505–3515.

(40) Pabst, T. P.; Quach, L.; MacMillan, K. T.; Chirik, P. J. Mechanistic Origins of Regioselectivity in Cobalt-Catalyzed $\text{C}(\text{sp}^2)$ -H Borylation of Benzoate Esters and Arylboronate Esters. *Chem.* **2021**, *7*, 237–254.

(41) Hall, D. *Boronic Acids: Preparation and Applications in Organic Synthesis, Medicine and Materials*; Wiley-VCH: Weinheim, Germany, 2011.

(42) Fasano, V.; McFord, A. W.; Butts, C. P.; Collins, B. S. L.; Fey, N.; Alder, R. W.; Aggarwal, V. K. How Big is the Pinacol Boronic Ester as a Substituent? *Angew. Chem., Int. Ed.* **2020**, *59*, 22403–22407.

(43) Hansch, C.; Leo, A.; Taft, R. W. A Survey of Hammett Substituent Constants and Resonance and Field Parameters. *Chem. Rev.* **1991**, *91*, 165–195.

(44) Murai, S.; Kakiuchi, F.; Sekine, S.; Tanaka, Y.; Kamatani, A.; Sonoda, M.; Chatani, N. Efficient catalytic addition of aromatic carbon-hydrogen bonds to olefins. *Nature* **1993**, *366*, 529–531.

(45) For selected examples of catalytic $\text{C}(\text{sp}^2)$ -H functionalization methods utilizing chelation strategies to afford *meta* selectivity, see: (a) Leow, D.; Li, G.; Mei, T.-S.; Yu, J.-Q. Activation of remote *meta*-C–H bonds assisted by an end-on template. *Nature* **2012**, *486*, 518–522. (b) Wan, L.; Dastbaravardeh, N.; Li, G.; Yu, J.-Q. Cross-Coupling of Remote *meta*-C–H Bonds Directed by a U-Shaped Template. *J. Am. Chem. Soc.* **2013**, *135*, 18056–18059. (c) Tang, R.-Y.; Li, G.; Yu, J.-Q. Conformation-induced remote *meta*-C–H activation of amines. *Nature* **2014**, *507*, 215–220. (d) Kuninobu, Y.; Ida, H.; Nishi, M.; Kanai, M. A *meta*-selective C–H borylation directed by a secondary interaction between ligand and substrate. *Nat. Chem.* **2015**, *7*, 712–717. (e) Wang, X.-C.; Gong, W.; Fang, L.-Z.; Zhu, L.-Z.; Zhu, R.-Y.; Li, S.; Engle, K. E.; Yu, J.-Q. Ligand-enabled *meta*-C–H activation using a transient mediator. *Nature* **2015**, *519*, 334–338.

(46) Matsubara, T.; Koga, N.; Musaev, D. G.; Morokuma, K. Density Functional Study on Activation of *ortho*-CH Bond in Aromatic Ketone by Ru Complex. Role of Unusual Five-Coordinated d^6 Metallacycle Intermediate with Agostic Interaction. *J. Am. Chem. Soc.* **1998**, *120*, 12692–12693.

(47) Zhang, X.; Kanzelberger, M.; Emge, T. J.; Goldman, A. S. Selective Addition to Iridium of Aryl C–H Bonds Ortho to Coordinating Groups. Not Chelation-Assisted. *J. Am. Chem. Soc.* **2004**, *126*, 13192–13193.

(48) Ishiyama, T.; Isou, H.; Kikuchi, T.; Miyaura, N. *Ortho*-C–H borylation of benzoate esters with bis(pinacolato)diboron catalyzed by iridium–phosphine complexes. *Chem. Commun.* **2010**, *46*, 159–161.

(49) Jover, J.; Maseras, F. Mechanistic Investigation of Iridium-Catalyzed C–H Borylation of Methyl Benzoate: Ligand Effects in Regioselectivity and Activity. *Organometallics* **2016**, *35*, 3221–3226.

(50) Roering, A. J.; Hale, L. V. A.; Squier, P. A.; Ringgold, M. A.; Wiederspan, E. R.; Clark, T. B. Iridium-Catalyzed, Substrate-Directed C–H Borylation Reactions of Benzylic Amines. *Org. Lett.* **2012**, *14*, 3558–3561.

(51) Campeau, L.-C.; Hazari, N. Cross-Coupling and Related Reactions: Connecting Past Success to the Development of New Reactions for the Future. *Organometallics* **2019**, *38*, 3–35.

(52) Ben-Ari, E.; Gandelman, M.; Rozenberg, H.; Shimoni, L. J. W.; Milstein, D. Selective C–H Activation of Haloarenes by an Ir(I) System. *J. Am. Chem. Soc.* **2003**, *125*, 4714–4715.

(53) (a) Ruiz-Castillo, P.; Buchwald, S. L. Applications of Palladium-Catalyzed C–N Cross-Coupling Reactions. *Chem. Rev.* **2016**, *116*, 12564–12649. (b) Ishiyama, T.; Murata, M.; Miyaura, N. Palladium-(0)-Catalyzed Cross-Coupling Reaction of Alkoxydiboron with Haloarenes: A Direct Procedure for Arylboronic Esters. *J. Org. Chem.* **1995**, *60*, 7508–7510.

(54) (a) Zhu, D.; Budzelaar, P. H. M. Binuclear Oxidative Addition of Aryl Halides. *Organometallics* **2010**, *29*, 5759–5761. (b) Zhu, D.; Korobkov, I.; Budzelaar, P. H. M. Radical Mechanisms in the

Reaction of Organic Halides with Diiminepyridine Cobalt Complexes. *Organometallics* **2012**, *31*, 3958–3971.

(55) Some thermochemical data for metal–halogen bond dissociation energies in soluble coordination compounds are available. See: Luo, L.; Li, C.; Cucullu, M. E.; Nolan, S. P. Organoruthenium Thermochemistry. Absolute Metal–Ligand Bond Disruption Enthalpies in the $(\eta^5\text{-C}_5\text{Me}_5)(\text{CO})_2\text{Ru-X}$ System ($X = \text{H, Cl, Br, I}$) and Thermodynamic Influences of Ancillary Ligand Variation on the Ru–X Bond Disruption Enthalpy. *Organometallics* **1995**, *14*, 1333–1338.

(56) Luo, Y.-R. *Comprehensive Handbook of Chemical Bond Energies*; CRC Press: Boca Raton, FL, 2007.

(57) For reviews on competition between C–H and C–F bond activation and selectivity considerations thereof, see ref 3g as well as: Clot, E.; Eisenstein, O.; Jasim, N.; Macgregor, S. A.; McGrady, J. E.; Perutz, R. N. C–F and C–H Bond Activation of Fluorobenzenes and Fluoropyridines at Transition Metal Centers: How Fluorine Tips the Scales. *Acc. Chem. Res.* **2011**, *44*, 333–348.

(58) Bosque, R.; Clot, E.; Fantacci, S.; Maseras, F.; Eisenstein, O.; Perutz, R. N.; Renkema, K. B.; Caulton, K. G. Inertness of the Aryl–F Bond toward Oxidative Addition to Osmium and Rhodium Complexes: Thermodynamic or Kinetic Origin? *J. Am. Chem. Soc.* **1998**, *120*, 12634–12640.

(59) Chin, R. M.; Dong, L.; Duckett, S. B.; Partridge, M. G.; Jones, W. D.; Perutz, R. N. Control of η^2 -Coordination vs C–H Activation by Rhodium: The Role of Aromatic Resonance Energies. *J. Am. Chem. Soc.* **1993**, *115*, 7685–7695.

(60) Fornies, J.; Green, M.; Spencer, J. L.; Stone, F. G. A. Synthesis and Some Oxidative-addition Reactions of Bis-(tricyclohexylphosphine)platinum. *J. Chem. Soc., Dalton Trans.* **1977**, 1006–1009.

(61) Cronin, L.; Higgitt, C. L.; Karch, R.; Perutz, R. N. Rapid Intermolecular Carbon–Fluorine Bond Activation of Pentafluoropyridine at Nickel(0): Comparative Reactivity of Fluorinated Arene and Fluorinated Pyridine Derivatives. *Organometallics* **1997**, *16*, 4920–4928.

(62) Reinhold, M.; McGrady, J. E.; Perutz, R. N. A Comparison of C–F and C–H Bond Activation by Zerovalent Ni and Pt: A Density Functional Study. *J. Am. Chem. Soc.* **2004**, *126*, 5268–5276.

(63) Ahrens, T.; Kohlmann, J.; Ahrens, M.; Braun, T. Functionalization of Fluorinated Molecules by Transition-Metal Mediated C–F Bond Activation To Access Fluorinated Building Blocks. *Chem. Rev.* **2015**, *115*, 931–972.

(64) Liu, W.; Welch, K.; Trindle, C. O.; Sabat, M.; Myers, W. H.; Harmon, W. D. Facile Intermolecular Aryl–F Bond Cleavage in the Presence of Aryl C–H Bonds: Is the η^2 -Arene Intermediate Bypassed? *Organometallics* **2007**, *26*, 2589–2597.

(65) Fan, L.; Parkin, S.; Ozerov, O. V. Halobenzenes and Ir(I): Kinetic C–H Oxidative Addition and Thermodynamic C–Hal Oxidative Addition. *J. Am. Chem. Soc.* **2005**, *127*, 16772–16773.

(66) Gatard, S.; Çelenligil-Çetin, R.; Guo, C.; Foxman, B. M.; Ozerov, O. V. Carbon–Halide Oxidative Addition and Carbon–Carbon Reductive Elimination at a (PNP)Rh Center. *J. Am. Chem. Soc.* **2006**, *128*, 2808–2809.

(67) Wu, H.; Hall, M. B. Carbon–hydrogen vs. carbon–halogen oxidative addition of chlorobenzene by a neutral iridium complex explored by DFT. *Dalton Trans.* **2009**, 5933–5942.

(68) Wu, H.; Hall, M. B. Kinetic C–H Oxidative Addition vs Thermodynamic C–X Oxidative Addition of Chlorobenzene by a Neutral Rh(I) System. A Density Functional Theory Study. *J. Phys. Chem. A* **2009**, *113*, 11706–11712.

(69) Hirsekorn, K. F.; Hulley, E. B.; Wolczanski, P. T.; Cundari, T. R. Olefin Substitution in $(\text{silox})_3\text{M}(\text{olefin})$ (silox) tBu_3SiO ; $\text{M} = \text{Nb, Ta}$): The Role of Density of States in Second vs Third Row Transition Metal Reactivity. *J. Am. Chem. Soc.* **2008**, *130*, 1183–1196.

(70) Rummelt, S. M.; Zhong, H.; Léonard, N. G.; Semproni, S. P.; Chirik, P. J. Oxidative Addition of Dihydrogen, Boron Compounds, and Aryl Halides to a Cobalt(I) Cation Supported by a Strong-Field Pincer Ligand. *Organometallics* **2019**, *38*, 1081–1090.